



Combined U–Pb, hafnium and oxygen isotope analysis of zircons from meta-igneous rocks in the southern North China Craton reveal multiple events in the Late Mesoarchean–Early Neoproterozoic

Dunyi Liu^{a,b}, Simon A. Wilde^{c,*}, Yusheng Wan^{a,b}, Shiyan Wang^d, John W. Valley^e, Noriko Kita^e, Chunyan Dong^{a,b}, Hangqiang Xie^{a,b}, Changxiu Yang^d, Yixin Zhang^d, Linzhi Gao^a

^a Institute of Geology, Chinese Academy of Geological Sciences, Beijing, 100037, China

^b Beijing SHRIMP Center, Beijing, 100037, China

^c Department of Applied Geology, Curtin University of Technology, Perth, Western Australia, 6845, Australia

^d Regional Geological Survey Party, Henan Bureau of Geology and Mineral Exploration and Development, Zhengzhou, 450001, Henan, China

^e Department of Geoscience, University of Wisconsin, Madison, WI 53706, USA

ARTICLE INFO

Article history:

Accepted 27 October 2008

Keywords:

Tonalite
Supracrustal rocks
Mesoarchean
SHRIMP dating
Hf isotopes
Oxygen isotopes
North China Craton

ABSTRACT

We report the results of a comprehensive isotopic investigation of zircons from metamorphosed tonalites and amphibolites from Lushan in the far south of the Trans-North China Orogen of the North China Craton that reveal the oldest rocks yet dated from the orogen. A detailed investigation of the internal structures of zircons, combined with targeted SIMS U–Pb and oxygen isotope analyses and ICP-MS Hf zircon analyses, has resulted in the discovery of previously unknown geological events in the North China Craton. Magmatic zircon from the tonalite and amphibolite was found to be essentially coeval with a small spread of ages from 2829 ± 18 Ma to 2832 ± 11 Ma in the tonalites and from 2838 ± 35 Ma to 2845 ± 23 Ma in amphibolite. Hafnium isotope data suggest derivation of both tonalite and amphibolite from a depleted mantle source with minor crustal contamination. Oxygen isotope ratios in zircons range from 5.1 to 7.3‰ VSMOW, with high $\delta^{18}\text{O}$ results recorded only from metamorphic domains. The earliest stage of metamorphic zircon growth, present in all four samples analyzed in this study, occurred between $2772 \pm 17/22$ in the tonalites and 2776 ± 20 and 2792 ± 12 Ma in the amphibolites. A younger metamorphic event at 2638 ± 61 in the tonalite and between 2671 ± 13 and 2651 ± 13 Ma in the amphibolites is recognized in zircons from three of the four samples investigated. This is the first time that metamorphic events at either of these times have been recorded in the North China Craton. Importantly, there is no evidence for the 1.8 Ga high-grade metamorphic event that is manifest in the northern and central parts of the Trans-North China Orogen.

© 2008 Elsevier B.V. All rights reserved.

1. Introduction

The North China Craton (NCC) has a long geological history, with the Neoproterozoic being the most important period of crustal formation (Kröner et al., 1998, 2005; Wilde et al., 2005; Wan et al., 2005a; Shen et al., 2005; Wu et al., 2005). Old rocks with ages from 3.8–3.3 Ga are recorded from the Eastern Block of the craton at Anshan (Jahn et al., 1987; Liu et al., 1992; Song et al., 1996; Wan et al., 2005b; Liu et al., 2007), whereas rocks with ages of ~2.7 Ga are also known from eastern and western Shandong Province in the extreme eastern segment of the Eastern Block (Fig. 1a) (Jahn et al., 1988, 2008). In the Trans-North China Orogen (Fig. 1a), rocks formed at ~2.8 Ga have rarely been identified, although several detrital and inherited zircons of this age have been recorded. However, Kröner et al. (1988) reported ~2.8 Ga zircon evaporation ages for tonalite in the Lushan area, Henan

Province, in the southern part of the orogen and interpreted them as the time of intrusion. There are also enclaves of supracrustal rocks, including amphibolite, in the tonalites, but their formation age was previously unknown. This is important, since the only other rocks of this age recorded from the Trans-North China Orogen are considerably further north in the Hengshan and Fuping complexes (Kröner et al., 2005) (4 and 5, respectively in Fig. 1a). Our aim in this study is to apply a range of modern micro-analytical techniques to zircons obtained from both amphibolites and meta-tonalites at Lushan. These include ICP-MS Hf and SIMS U–Pb and oxygen isotope analyses of various zircon domains identified by detailed cathodoluminescence study, in order to resolve their crystallization age and subsequent metamorphic history.

2. Geological background and sample selection

Lushan is located in the southern portion of the Trans-North China Orogen (Fig. 1a, b), where early Precambrian basement is in faulted or

* Corresponding author.

E-mail address: s.wilde@curtin.edu.au (S.A. Wilde).

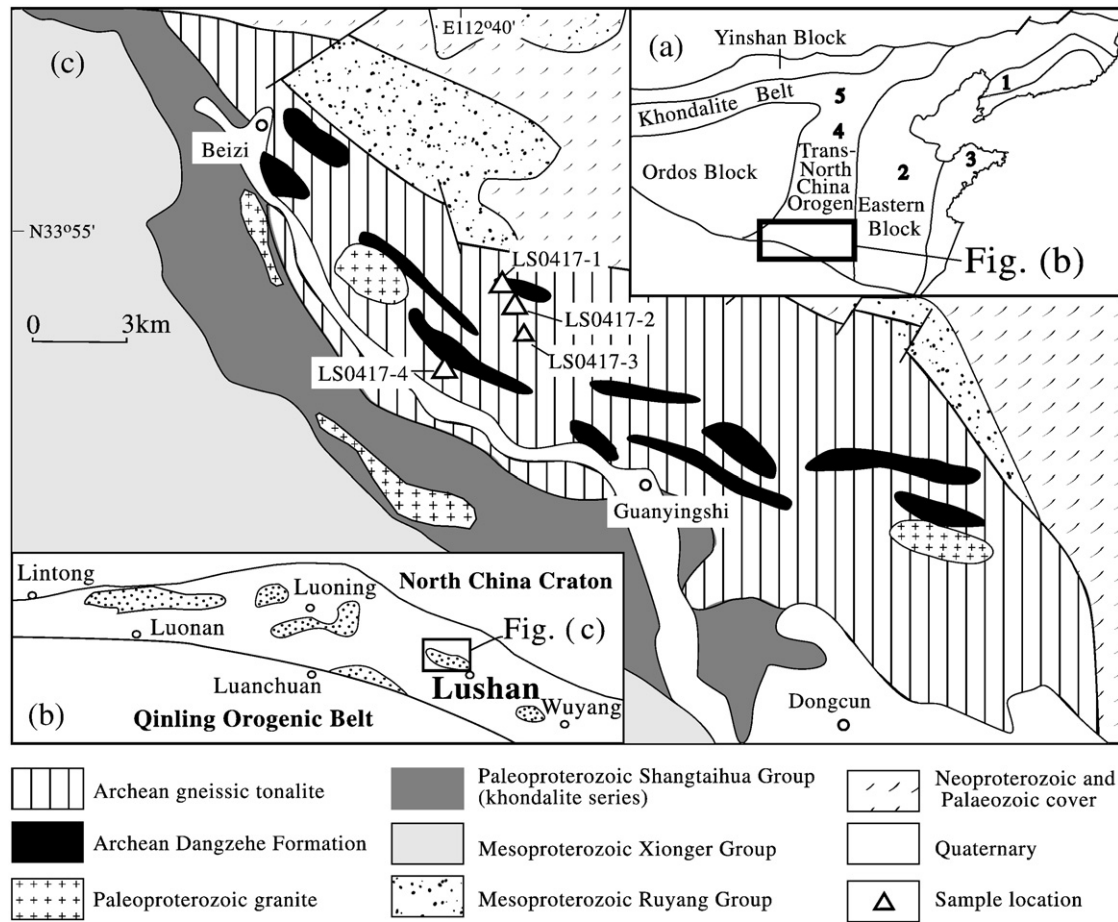


Fig. 1. (a) Major tectonic subdivisions of the North China Craton (from Zhao et al., 2005), 1-Anshan; 2-western Shandong Province; 3-eastern Shandong Province; 4-Fuping; 5-Hengshan. (b) Rock outcrop distribution map for the southern part of the Trans-North China Orogen. (c) Geological map of rocks in the Lushan area (modified after Yang, 2008) showing sample locations.

unconformable contact with the Mesoproterozoic Ruyang Group and Neoproterozoic and Paleozoic cover in the northeast, and is unconformably overlain by the Mesoproterozoic Xionger Group in the southwest (Fig. 1c). The basement rocks have undergone strong metamorphism and deformation and were named the Taihua Group, which was further subdivided into the Xiataihua and Shangtaihua sub-groups (Lower and Upper Taihua groups, respectively). Zhang et al. (1985) established that the majority of the Xiataihua Group consists of tonalitic gneisses, which are geochemically similar to those in other high-grade terranes of the world. These authors considered that all the basement rocks formed during the same period (Late Archean). However, Kröner et al. (1988) suggested that the tonalitic gneisses formed during the Mesoarchean, based on zircon evaporation ages of ~2.8 Ga. Conversely, Hu et al. (1988) and Chen et al. (1996) considered that the Shangtaihua Group formed during the Paleoproterozoic. The latter view was supported by Wan et al. (2006b), who obtained the youngest detrital zircon age of ~2.3 Ga and metamorphic zircon ages of 1.84 Ga for graphite–garnet–sillimanite gneiss from the Shangtaihua Group (note that ‘Group’ in China has previously been used loosely to describe discrete packages of rocks and does not always conform to the international stratigraphic nomenclature; throughout this paper, we identify these using the notation “group”, following the discussion in Wan et al., 2006b).

The Shangtaihua “group” is mainly composed of graphite-bearing gneiss, marble, banded iron formation (BIF) and amphibolite that underwent amphibolite to granulite metamorphism (Wan et al., 2006b; Yang, 2008), with characteristics similar to the khondalite series of Southern India (Dash et al., 1987; Chacko et al., 1992). The gneissic tonalites contain slices and enclaves of dismembered

supracrustal rocks of various sizes (Fig. 1c), with rafts up to several kilometres in length. The supracrustal rocks consist mainly of amphibolite, (garnet-bearing) hornblende-plagioclase gneiss and biotite-plagioclase gneiss. Some sillimanite-kyanite gneiss and marble also occur within the tonalites (Yang, 2008), but their relationship is unclear (whether enclaves or tectonic slices). Some amphibolites are banded, due mainly to variations in plagioclase and hornblende content, and they appear to be of volcano-sedimentary origin (Fig. 2a). The tonalites (Fig. 2b, c) commonly show strong deformation fabrics and can be broadly subdivided into two types: hornblende tonalite and biotite tonalite. They differ in their biotite and hornblende contents and the contacts between them are commonly gradational. Locally, the biotite tonalites underwent anatexis (Fig. 2b).

Two supracrustal rock samples were collected for detailed zircon analysis. A banded amphibolite (LS0417-1) was obtained from a huge enclave in the tonalite at N33°55'21", E112°40'52" (Figs. 1c and 2a). It is composed mainly of plagioclase (45%) and amphibole (50%), with minor diopside (<5%) and accessory opaque minerals. The second sample is a quartz-plagioclase-hornblende gneiss (LS0417-3) collected from N33°54'23", E112°41'14", which has a strong deformation fabric and consists of amphibole (60%), plagioclase (15%) and quartz (25%), with trace zircon and opaque minerals.

Two tonalite samples were selected for zircon analysis based on differences in their mineralogy. Sample LS0417-2 is a gneissic biotite tonalite collected from N33°54'56", E112°41'13" (Figs. 1c and 2b) and composed of plagioclase (60%), quartz (30%), biotite (7%) and hornblende (3%). The rock is extensively cut by granitic veins that pinch-out along strike (Fig. 2b) and appear to be of local, anatexitic origin; these were carefully excluded from the analyzed material.

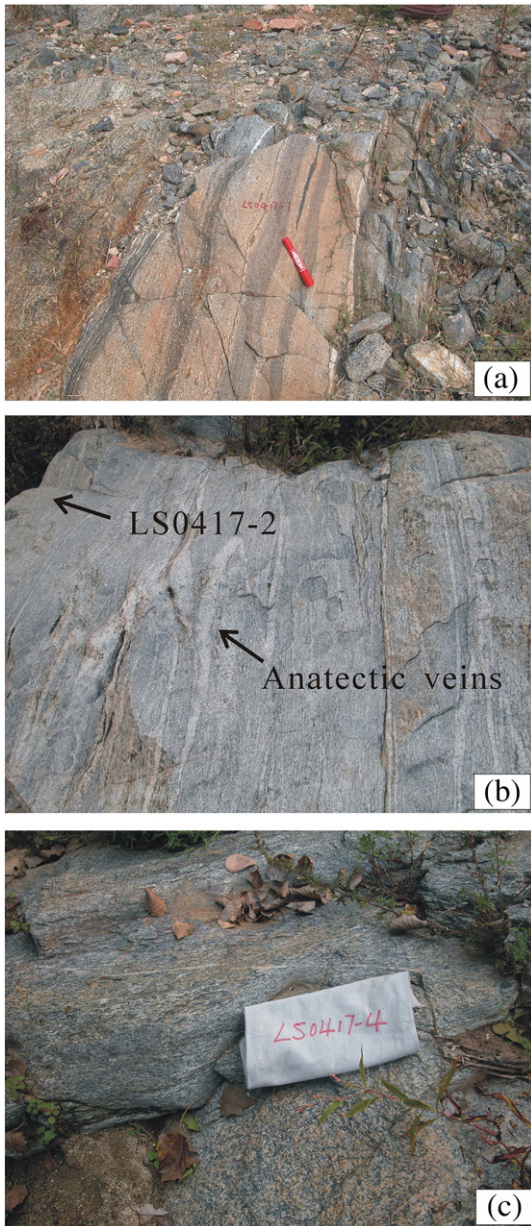


Fig. 2. Field photographs of outcrops sampled in the Lushan area: (a) Banded amphibolite (LS0417-1), the pen is 14 cm long; (b) Gneissic biotite tonalite (LS0417-2) cut by thin anatectic veins, field of view is 1.3 m wide; (c) Gneissic hornblende tonalite (LS0417-4), the sample bag is 35 cm wide.

Sample LS0417-4 was obtained from N33°53'52", E112°39'48" (Figs. 1c and 2c) and is richer in hornblende, being composed of plagioclase (65%), hornblende (20%) and quartz (15%), with traces of biotite.

3. Analytical techniques

Rock samples were crushed following standard procedures and then powdered in an agate mill to 200-mesh for geochemical analysis. Major oxides were analyzed by XRF on a Rigaku 3080E using fused glass beads, with FeO determined separately by the standard Penfield tube method of wet chemical analysis. Trace elements were determined using a VG Elemental® PQ Excell ICP-MS, both instruments located at the Institute of Geological Analysis, Chinese Academy of Geological Science (CAGS). For trace element analyses, the fused glass beads were powdered and dissolved using an HF/HNO₃ (1:1) mixture in screw-top Teflon beakers for 12 h at ~100 °C, followed by evaporation to dryness. They were then refluxed in 7N HNO₃ for >12 h at ~100 °C and finally diluted with 2%

HNO₃. The Chinese domestic granite standard GSR-1 was used to calibrate and monitor the analytical data, and its recommended values and mean measured values during the sessions are shown in Table 1. The relative standard deviations (RSD) of major oxides and rare earth elements are mostly less than 5% and 8%, respectively (Table 1).

Zircons were extracted from separate crushed fractions of the samples using a combination of heavy liquid and magnetic techniques. The crystals were hand picked under a binocular microscope, mounted in epoxy resin discs and then polished until all mineral grains were cut approximately to their mid-sections. The grains were imaged using cathodoluminescence (CL) techniques in order to determine their internal structure prior to analysis. Mineral inclusions were identified using a Jasco nitrogen Raman spectroscopy with a Renishaw 1000 laser using the 514.5 nm line and their compositions determined at the Institute of Mineral Resources, CAGS, using a Jeol JXA 8800R electron microprobe with 20 kV accelerating voltage and 2.1 nA beam current. Dating of zircons was carried out using the SHRIMP II ion microprobe at the Beijing SHRIMP Centre, CAGS. Analytical procedures are similar to those described by Williams (1998) and Wan et al. (2005c). Mass resolution during the analytical sessions was ~5000 (1% peak height). The intensity of the primary O⁻² ion beam was 5–6 nA. Spot sizes were ~30 μm and each site was rastered for 150 s prior to analysis to remove contamination from the gold coating. Five scans through the mass stations were made for each age determination. The calibration standard used was SL13, with an age of 572 Ma and U content of 238 ppm (Williams, 1998), whereas TEM, with an age of 417 Ma (Black et al., 2003), was used to monitor performance. The ratio of TEM standard analyses to sample analyses was 1:3–4 and the uncertainty of the mean Pb/U calibration constant over the various analytical sessions was <1.7% (2σ). Decay constants used for age calculation are those recommended by the IUGS Subcommittee on Geochronology (Steiger and Jaeger, 1977). The common lead correction was applied using the measured ²⁰⁴Pb abundances and assuming Broken Hill lead composition. Data processing was carried out using the SQUID and ISOPLOT programs (Ludwig, 2001a,b). The uncertainties in Table 1 and on the concordia diagrams for individual analyses are quoted at the 1σ level, whereas the errors on weighted mean ages given in Fig. 6 and in the text are quoted at the 95% confidence level.

Oxygen isotope analyses were performed on a CAMECA ims-1280 large radius, multi-collector ion microprobe at Wisc-SIMS, University of Wisconsin – Madison. A ¹³³Cs⁺ primary ion beam was defocused to a diameter of 10 μm with sample current of ~2 nA. Secondary O⁻ ions were accelerated by –10 kV with a normal-incidence electron gun for charge compensation. The secondary optics were similar to those described in Kita et al. (2007) and Page et al. (2007). The intensity of ¹⁶O was ~2 × 10⁹ cps and the mass resolving power was ca. 2500, sufficient to separate hydride interferences on ¹⁸O. Two multi-collector Faraday Cups (FC) were used to measure ¹⁶O and ¹⁸O simultaneously, equipped with different amplifiers (10¹⁰ and 10¹¹ Ω resistors, respectively). The base line of the FC amplifiers was calibrated every 12 h; drift during the day was insignificant compared to the noise level of the detectors (≤1000 cps for FC with 10¹¹ Ω resistor). Magnet control was by NMR probe with stability better than 10 ppm/10 h. At each analysis position, any small misalignment of the secondary optics due to changing stage position was automatically re-tuned before each analysis. Data were corrected for instrumental mass fractionation (IMF) using fragments of the zircon standard 91500 (Wiedenbeck et al., 2004) mounted in the sample block. Standards were measured four times every 10–20 sample analyses and the average value of IMF of the total 8 standard analyses that bracket the sample analyses was used as the IMF correction. The external error of 14 standard analyses is 0.3% 2SD (2SE = 0.08‰) and represents the spot-to-spot precision of this technique. Oxygen isotope ratios are reported in standard permil notation relative to Vienna Standard Mean Ocean Water (VSMOW).

Table 1
Geochemical data for Archean rocks in the Lushan area and standard GSR-1.

Sample no.	LS0417-1	LS0417-3	LS0417-2	LS0417-4	Standard GSR-1 (granite)		
	Banded amphibolite	Gneissic amphibolite	Gneissic biotite tonalite	Gneissic hornblende–biotite tonalite	Recommended values	Mean measured value (n = 10)	RSD (%)
SiO ₂	49.85	64.11	67.63	60.64	72.83 ± 0.10	72.88	0.22
TiO ₂	0.86	0.78	0.45	0.58	0.29 ± 0.03	0.29	5.50
Al ₂ O ₃	14.60	11.38	15.95	15.93	13.40 ± 0.07	13.43	0.71
Fe ₂ O ₃	3.01	1.88	1.45	1.88	1.02 ± 0.06	1.03	4.44
FeO	6.74	3.23	2.53	3.52	1.02 ± 0.04	1.03	3.55
MnO	0.20	0.05	0.07	0.08	0.06 ± 0.001	0.06	0.00
MgO	4.74	12.01	1.49	3.91	0.42 ± 0.04	0.42	9.31
CaO	16.07	1.20	4.11	6.01	1.55 ± 0.05	1.59	1.25
Na ₂ O	1.73	1.47	4.62	4.88	3.13 ± 0.06	3.07	1.75
K ₂ O	0.62	0.18	1.31	0.94	5.01 ± 0.07	5.11	2.44
P ₂ O ₅	0.09	0.18	0.13	0.31	0.09 ± 0.001	0.09	11.98
H ₂ O ⁺	1.14	3.10	0.54	1.10	0.60 ± 0.05	0.62	4.74
LOL	2.16	2.98	0.46	1.12	~0.70	0.74	2.70
Total	101.81	102.55	100.74	100.90			
La	8.54	4.69	30.0	27.3	54 ± 4	53.3	5.83
Ce	21.4	10.6	55.6	67.5	108 ± 7	105	4.79
Pr	2.93	1.70	6.18	9.09	12.7 ± 0.8	12.0	5.77
Nd	12.5	8.09	21.6	37.9	40 ± 3	42.5	6.21
Sm	3.36	2.33	3.57	6.57	9.7 ± 0.8	9.26	8.67
Eu	1.13	0.59	1.00	1.86	0.85 ± 0.07	0.82	11.60
Gd	3.71	2.19	2.14	4.22	9.3 ± 0.7	9.27	6.02
Tb	0.68	0.35	0.30	0.49	1.65 ± 0.09	1.70	10.53
Dy	4.28	2.24	1.48	2.30	10.2 ± 0.4	10.3	7.50
Ho	0.90	0.46	0.26	0.39	2.05 ± 0.17	2.18	7.10
Er	2.69	1.31	0.67	1.10	6.5 ± 0.3	6.5	6.84
Tm	0.37	0.20	0.08	0.13	1.06 ± 0.09	1.09	5.00
Yb	2.37	1.20	0.45	0.79	7.4 ± 0.5	7.69	4.70
Lu	0.36	0.19	0.07	0.12	1.15 ± 0.09	1.20	3.69
ΣREE	65.2	36.1	123.4	159.8			
(La/Yb) _n	2.4	2.6	43.9	22.8			
Eu/Eu*	0.98	0.79	1.03	1.02			

Note: Major oxides in wt.%, trace elements in ppm.

The *in-situ* Lu–Hf isotopic analysis of zircon was carried out using the Neptune multi-collector ICP-MS at the State Key Laboratory of Lithospheric Evolution, Institute of Geology and Geophysics, Chinese Academy of Sciences in Beijing. A 193 nm UV ArF excimer laser ablation system was used for laser ablation analysis. Instrumental conditions and analytical procedures are described in Wu et al. (2006). Ablation times were about 26 s for 200 cycles of each measurement, with a 6 Hz repetition rate, a laser power of 100 mJ/pulse and a spot size of 63 μm. The zircon standard used was 91500 (¹⁷⁶Hf/¹⁷⁷Hf = 0.282306; Woodhead et al., 2004). The errors for the Lu–Hf isotope results are quoted at the 95% confidence level. The calculation of Hf model ages was based on a depleted-mantle source with a present-day ¹⁷⁶Hf/¹⁷⁷Hf = 0.28325 (Griffin et al., 2000), using the ¹⁷⁶Lu

decay constant $1.865 \times 10^{-11} \text{ year}^{-1}$ (Scherer et al., 2001). The calculation of $\varepsilon_{\text{Hf}(T)}$ values was based on zircon SHRIMP U–Pb ages and the chondritic values (¹⁷⁶Hf/¹⁷⁷Hf = 0.282772, ¹⁷⁶Lu/¹⁷⁷Hf = 0.0332; Blichert-Toft and Albarede, 1997).

4. Whole-rock geochemistry

4.1. Supracrustal rocks

Banded amphibolite sample LS0417-1 was sliced into separate light and dark portions and only the grey (lighter) part was analyzed, although both the grey and dark bands were prepared for zircon separation (Figs. 1c and 2a). The grey portion (Table 1) is similar in major element composition to tholeiite, but higher in CaO (16.07%). It also has a REE composition similar to tholeiite, with ΣREE, Eu/Eu* and (La/Yb)_n being 65.2 ppm, 0.98 and 2.4, respectively (Table 1; Fig. 3). The quartz-plagioclase-hornblende gneiss sample (LS0417-3) has high MgO (12.01%) and SiO₂ (64.11%) and low ΣFeO (FeO + 0.9 × Fe₂O₃, 4.92%), CaO (1.20%), Na₂O (1.47%) and K₂O (0.18%). It has lower ΣREE contents than LS0417-1 (Table 1; Fig. 3). The mineral association and chemical composition suggest that its protolith is of volcano-sedimentary origin.

4.2. Tonalites

Biotite tonalite LS0417-2 has higher SiO₂ and lower ΣFeO, MgO and CaO than hornblende tonalite LS0417-4 (Table 1), consistent with its lower amphibole content. Both samples have moderate REE contents (ΣREE = 123–160 ppm), small positive Eu-anomalies (Eu/Eu* = 1.02–1.03) and strongly fractionated REE patterns ((La/Yb)_n = 22.8–43.9) (Table 1; Fig. 3). Geochemically, they are in the range of most reported Archean tonalite–trondhjemite–granodiorite rocks

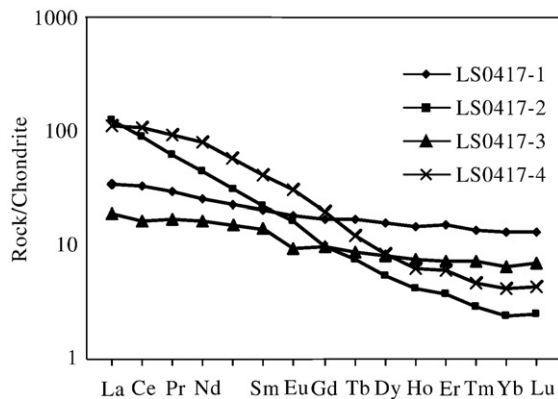


Fig. 3. Chondrite-normalized REE patterns of rocks from the Lushan area. Normalization values are from Sun and McDonough (1989).

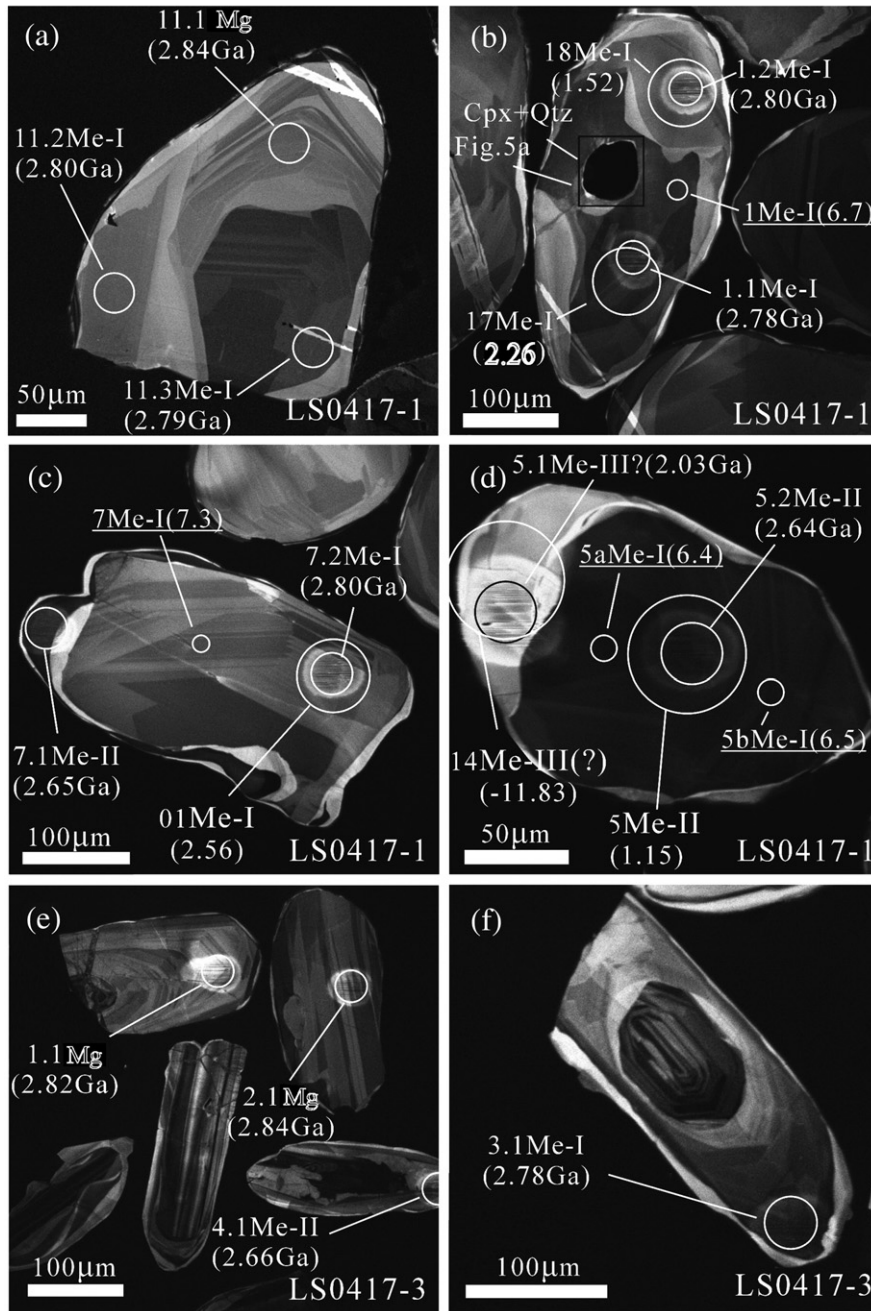


Fig. 4. Zircon cathodoluminescence images: (a), (b), (c) and (d) banded amphibolite (LS0417-1); (e) and (f) gneissic amphibolite (LS0417-3). Circles (~ 60 , ~ 30 , and ~ 10 μm) show positions of Lu–Hf, SHRIMP U–Pb and O analytical sites, respectively, with their identification numbers as in Tables 3–5. In brackets after the Lu–Hf site numbers are the $\epsilon_{\text{Hf}}(T)$ values, after the SHRIMP site numbers the $^{207}\text{Pb}/^{206}\text{Pb}$ ages and after the O site numbers the $\delta^{18}\text{O}$ values. Mg, Me-I, and Me-II represent magmatic zircon and first and second event metamorphic zircon domains, respectively. In Fig. 4b, Cpx = clinopyroxene and Qtz = quartz.

(TTGs) (Arth and Hanson, 1975; Jahn et al., 1981; Martin et al., 2005). The strong REE fractionation is attributed to partial melting of a basaltic source, leaving garnet and hornblende as residual phases.

5. Zircon characteristics and U–Pb ages

5.1. Supracrustal rocks

5.1.1. Banded amphibolite (LS0417-1)

Zircons from this sample are stubby or rounded in shape with length to width ratios of 1.5–2:1. Magmatic zircons with oscillatory zoning in cathodoluminescence (CL) image are rarely present (Fig. 4a) and only two analyses (labeled ‘Mg’ in Fig. 4a) could be obtained. They

give a weighted mean $^{207}\text{Pb}/^{206}\text{Pb}$ age of 2838 ± 35 Ma (MSWD = 0.01) and have low U (42 and 61 ppm) and Th (8 and 23 ppm) contents and Th/U ratios of 0.21 and 0.39, respectively. However, most zircons show fir-tree and banded structures in CL image (Fig. 4a, b, c, d), similar to features interpreted to form under high-grade metamorphic conditions (upper amphibolite and granulite facies; Vavra et al., 1996). Inclusions of pyroxene, amphibole, Ca-rich feldspar, quartz and apatite are present in these domains. (Table 2; Fig. 5a, b). Thirteen SHRIMP U–Pb analyses were made, designated here as ‘Me-I’. Their U and Th contents and Th/U ratios range from 46–180 ppm, 9–102 ppm, and 0.19–0.68, respectively (Table 3). All analyses are distributed on or about concordia (Fig. 6a), with a weighted mean $^{207}\text{Pb}/^{206}\text{Pb}$ age of 2792 ± 11 Ma (MSWD = 0.21). The Me-I zircons commonly show

Table 2

Compositions of inclusions within zircons from banded amphibolite (LS0417-1) in the Lushan area.

	1	2	3	4	5	6
	LS0417-1-1Cpx	LS0417-1-2Cpx	LS0417-1-5Cpx	LS0417-1-3Hb	LS0417-1-4Hb	LS0417-1-6Pl
SiO ₂	51.23	49.95	49.95	44.05	43.77	53.84
TiO ₂	0.19	0.26	0.23	1.13	1.16	0.03
Al ₂ O ₃	1.10	2.64	2.59	10.83	10.81	27.72
FeO	11.78	13.09	12.38	17.31	17.27	0.04
MgO	10.70	9.63	10.07	10.56	10.37	–
MnO	0.46	0.38	0.40	0.30	0.27	–
CaO	23.46	22.85	22.77	11.43	11.32	10.68
Na ₂ O	0.45	0.55	0.64	1.62	1.50	5.08
K ₂ O	0.02	0.01	0.13	0.90	0.94	0.16
Cr ₂ O ₃	0.06	0.02	0.08	0.16	0.15	–
NiO	0.01	0.00	0.00	0.04	0.02	–
H ₂ O	–	–	–	1.67	2.42	–
Total	99.45	99.37	99.24	100.00	100.00	97.54

Note: 1) Cpx, Hb and Pl refer to clinopyroxene, hornblende and plagioclase, respectively. 2) All these inclusions occur in domains formed during the first episode of metamorphism (Me-I).

overgrowth rims (labeled 'Me-II' in Table 3 and Fig. 4c), which are dark in CL and usually narrow in width. One zircon grain also has similar characteristics and age to the overgrowth rims (grain 5 in Fig. 4d), so this is likewise classified as 'Me-II' type zircon. Seven analyses on the Me-II domains define a weighted mean ²⁰⁷Pb/²⁰⁶Pb age of 2651 ± 13 Ma (MSWD = 0.87). Their U and Th contents and Th/U ratios range from 106–412 ppm, 4–17 ppm and 0.02–0.08, with the exception of 8.1Me-II which has a Th/U ratio of 0.32 (Table 2). These results are taken to indicate that there was formation of metamorphic zircon at ~2650 Ma. It is interesting to note that grain 5 has an overgrowth rim ('Me-III' on Fig. 4d), which has a low Th/U ratio (0.02) and a ²⁰⁷Pb/²⁰⁶Pb age of 2032 ± 78 Ma (Table 3; Fig. 6a), much younger than the Me-II zircon domains, suggesting a metamorphic episode in the mid-Paleoproterozoic.

5.1.2. Gneissic amphibolite (LS0417-3)

This sample contains more abundant columnar magmatic zircon than LS0417-1, with length to width ratios of 2–3:1. Although zircons from the two samples are different in shape and structure, they record a similar history. Magmatic zircons from sample LS0417-3 (also identified as 'Mg' in Table 3 and Fig. 4) show banded or oscillatory zoning (Fig. 4e). Three analyses have U and Th contents and Th/U ratios of 40–106 ppm, 64–157 ppm and 1.1–2.4 and record a weighted mean ²⁰⁷Pb/²⁰⁶Pb age of 2845 ± 23 Ma (MSWD = 0.49) (Fig. 6b). Me-I overgrowth rims are more luminescent in CL (Fig. 4f) than in sample

LS0417-1 and a total of 5 analyses yield a weighted mean ²⁰⁷Pb/²⁰⁶Pb age of 2776 ± 20 Ma (MSWD = 0.41) (Fig. 6b). Their U and Th contents and Th/U ratios range from 35–126 ppm, 21–379 ppm and 0.62–3.12, respectively (Table 2). Similar to zircons from sample LS0417-1, Me-II domains are dark in CL and have high U and Th contents (101–937 ppm and 82–535 ppm), but they differ from the Me-II domains of zircons from sample LS0417-1 in also having high Th/U ratios (0.59–0.95) (Table 3). Four analyses on Me-II domains define a discordia line, with an upper intercept age of 2671 ± 25 Ma (MSWD = 0.51) (Fig. 6b).

5.2. Tonalitic rocks

5.2.1. Gneissic biotite tonalite (LS0417-2)

Zircons from this sample are columnar or stubby in shape, have length to width ratios of 1.5–3:1, and show core-rim structures in CL images, with the cores displaying prominent oscillatory zoning (labeled 'Mg' in Fig. 7a, b), consistent with a magmatic origin. The rims are commonly structureless or have banded and/or sector zoning in CL (Fig. 7a, b), being similar to 'Me-I' domains in zircons from the amphibolite samples. However, no dark rims have been identified like the 'Me-II' domains in the amphibolite zircons. Twenty-five analyses were made on 20 zircons and fourteen analyses of magmatic zircons have U contents of 35–666 ppm, Th contents of 22–193 ppm and Th/U ratios of 0.18–0.97 (Table 3). Nine of these give a weighted mean ²⁰⁷Pb/²⁰⁶Pb age of 2829 ± 18 Ma (MSWD = 1.50). Some zircons with magmatic

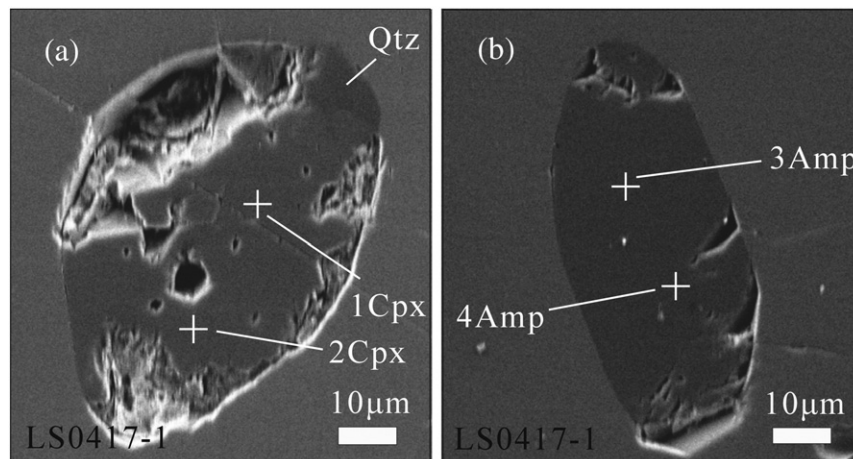


Fig. 5. Sites of mineral inclusions in zircons from banded amphibolite (LS0417-1) in the Lushan area in backscattered secondary electron images. Cpx, Qtz and Amp represent clinopyroxene, quartz and hornblende, respectively. See Fig. 4(b) for location of inclusion in Fig. 5(a).

zoning have similar ages to the rims (Fig. 6c). Eleven analyses on Me-I overgrowth rims have U contents of 20–90 ppm, Th contents of 24–188 ppm and Th/U ratios of 0.61–7.07 (with the latter value (Table 3) being extremely high). Of these, nine analyses yield a weighted mean $^{207}\text{Pb}/^{206}\text{Pb}$ age of 2772 ± 22 Ma (MSWD = 0.53) (Fig. 6c).

5.2.2. Gneissic hornblende–biotite tonalite (LS0417-4)

The zircons from this sample are columnar, stubby or irregular in shape, with length to width ratios of 1–2:1, and show complex structures in CL images including magmatic cores with oscillatory zoning (labeled 'Mg' in Fig. 7c, d, e, f). Unlike zircons from sample LS0417-1, the dark domains have similar ages to the grey domains with fir-tree and banded zoning (Fig. 7d, e). This suggests that both domains (composing Me-I) formed as a result of overgrowth or recrystallization of the magmatic cores during one and the same metamorphic event. Me-II domains form white or grey rims in CL, but only a few are wide enough to analyze (Fig. 7e, f). Eighteen analyses of magmatic zircons have U contents of 46–604 ppm, Th contents of 12–127 ppm and Th/U ratios of 0.22–1.16 (Table 3). They yield a weighted mean $^{207}\text{Pb}/^{206}\text{Pb}$ age of 2832 ± 11 Ma (MSWD = 1.10) after excluding four spots (7.1 Ma, 9.2 Mg, 12.2 Mg and 14.1 Mg) (Fig. 6d), thus being comparable in age to similar domains in sample LS0417-2. A total of 11 analyses were made on Me-I zircon domains which show a large variation in their U and Th contents (18–543 and 6–524 ppm, respectively) and Th/U ratios (0.08–5.15) (Table 3). Excluding analysis 6.1Me-I which is more discordant, the remaining analyses record a weighted mean $^{207}\text{Pb}/^{206}\text{Pb}$ age of 2772 ± 17 Ma (MSWD = 1.90). Three

analyses on Me-II domains have U and Th contents and Th/U ratios ranging from 18 to 25 ppm, 2–144 ppm and 0.08–0.55, respectively (Table 3). They yield an imprecise weighted mean $^{207}\text{Pb}/^{206}\text{Pb}$ age of 2638 ± 61 Ma (MSWD = 0.23) (Fig. 6d).

6. Oxygen isotope ratios of zircons

A total of 30 analyses were made for $\delta^{18}\text{O}$ on 29 zircons from samples LS0417-1, LS0417-2 and LS0417-4. Based on an evaluation of the U–Pb data and CL images, only the most unambiguous sites were selected for analysis. Taken as a whole, the recorded $\delta^{18}\text{O}$ values are typical of those found worldwide in igneous zircons of Archean age, ranging from 5.1 to 7.3‰ (Valley et al., 2005). For banded amphibolite sample LS0417-1, all analyses on metamorphic zircon domains range from 6.4 to 7.3‰ (Table 4), with an average of $6.8 \pm 0.5\%$ (Fig. 8a). Those obtained from Me-I sites ($n=5$) range from 6.7 to 7.3‰ and those from Me-II sites ($n=3$) from 6.4 to 7.0‰, indicating a virtually identical range. These mildly elevated values are consistent with their metamorphic origin, a conclusion drawn from the structure seen in CL images and the nature of the mineral inclusions (Table 2; Fig. 5). All analyses but one in samples LS0417-2 and LS0417-4 are on magmatic zircon domains and range in $\delta^{18}\text{O}$ value from 5.1 to 5.9‰ (Table 4; Fig. 8b, c), with an average of $5.7 \pm 0.4\%$ (2SD), the same as for zircons from TTGs and other unenriched igneous rocks of broadly the same age in the Superior Province of Canada ($5.5 \pm 0.4\%$, King et al., 1998). Values of $\delta^{18}\text{O} = 5.3 \pm 0.6\%$ are generally found in zircons from primitive, mantle-derived magmas (Valley et al., 2005). One analysis

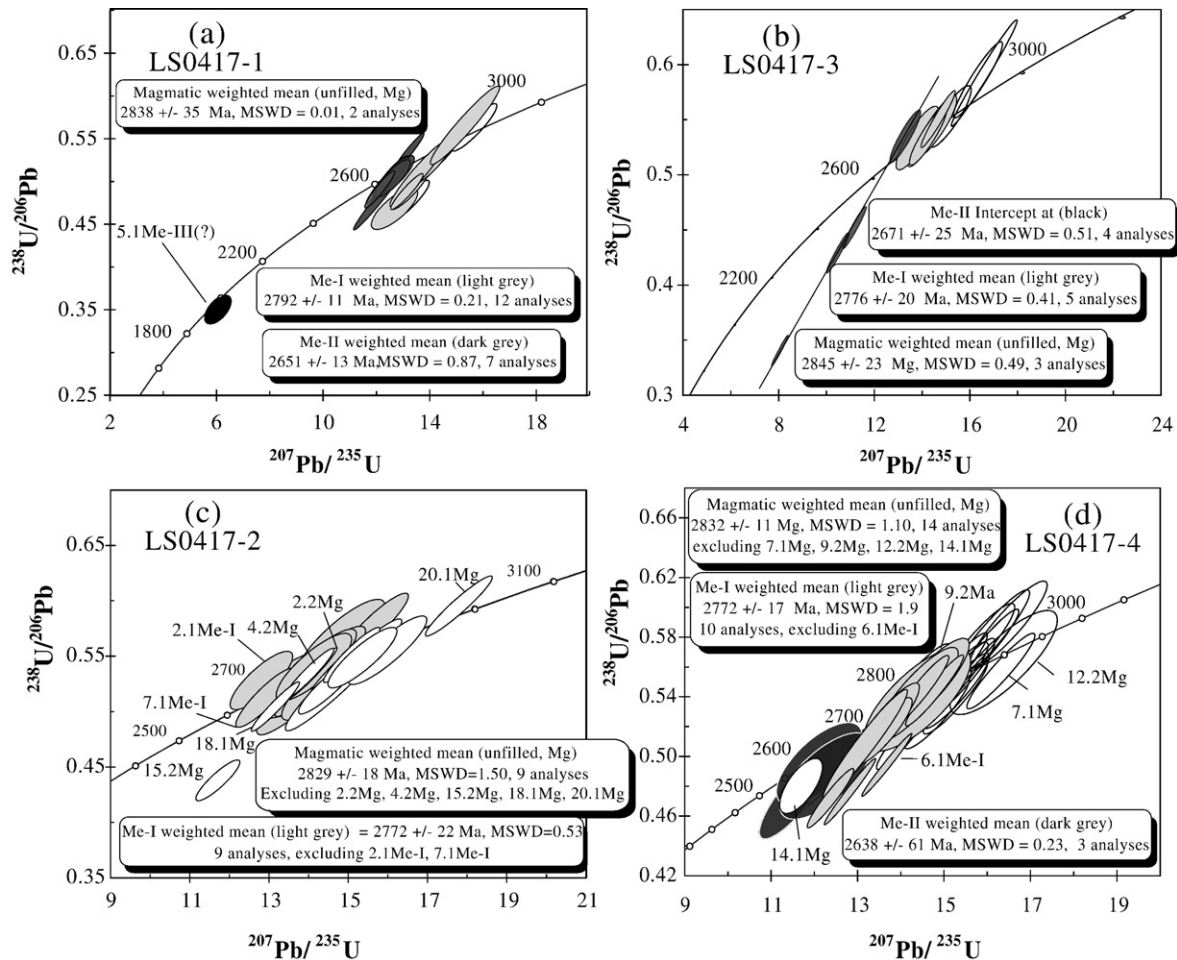


Fig. 6. Concordia diagrams of SHRIMP U–Pb data: (a) banded amphibolite (LS0417-1); unfilled, magmatic core; light grey, Meta-I; dark grey, Meta-II; (b) gneissic amphibolite (LS0417-3): unfilled, magmatic core; light grey, Meta-I; dark grey, Meta-II; (c) gneissic biotite tonalite (LS0417-2): unfilled, magmatic core; light grey, Meta-I; (d) gneissic hornblende–biotite tonalite (LS0417-4): unfilled, magmatic core; light grey, Meta-I; dark grey, Meta-II. Error ellipses are at the 1σ level.

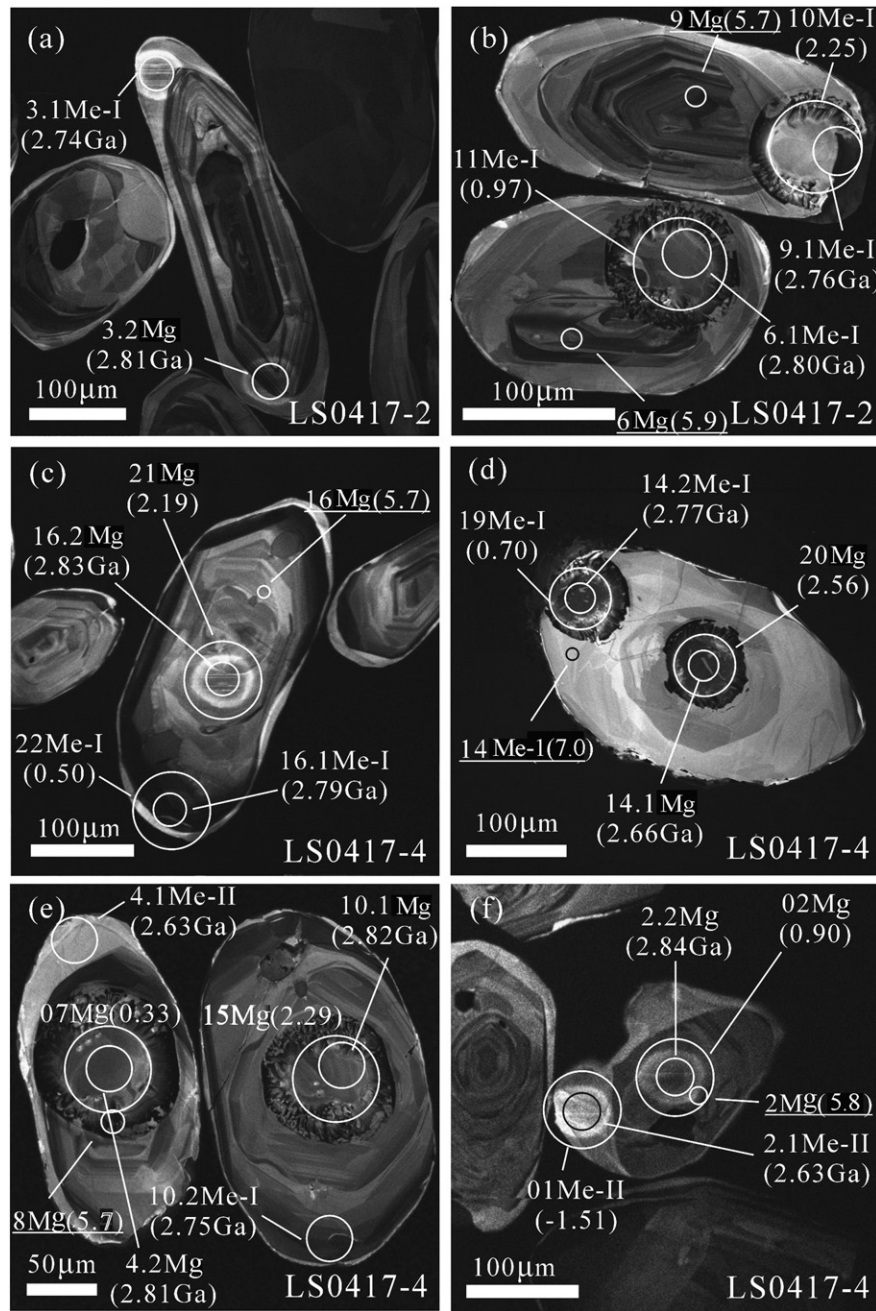


Fig. 7. Zircon cathodoluminescence images: (a) and (b) gneissic biotite tonalite (LS0417-2); (c), (d), (e) and (f) gneissic hornblende-biotite tonalite (LS0417-4). Circles (~60, ~30 and ~50 μm) show positions of Lu–Hf, SHRIMP U–Pb and O analytical sites, respectively, with their identification numbers as in Tables 3–5. In brackets after the Lu–Hf site numbers are the $\epsilon\text{Hf}(T)$ values, after the SHRIMP site numbers the $^{207}\text{Pb}/^{206}\text{Pb}$ ages and after the O site numbers the $\delta^{18}\text{O}$ values. Mg, Me-I, and Me-II represent magmatic, first and second metamorphic zircon domains, respectively. The disturbed pattern in some images is the result of ICP-MS laser ablation analyses for hafnium.

(#14) on the metamorphic rim of a zircon grain from sample LS0417-4 has a $\delta^{18}\text{O}$ value of 7.0‰ (Table 4; Figs. 7d and 8c), being significantly higher than the magmatic zircon values (Fig. 8c) and equivalent to data obtained from the metamorphic rims in banded amphibolite sample LS0417-1 (Fig. 8a).

7. Hf isotope compositions of the zircons

In order to assess the nature of the mantle source regions of the coeval amphibolites and meta-tonalites, we carefully selected a range of zircons from both suites that were well characterized by their CL patterns. In addition, we wished to test for any effects of the various

high-grade metamorphic events on the zircon Lu–Hf system, particularly in the light of the elevated $\delta^{18}\text{O}$ oxygen values obtained from the metamorphic rims. Analyses were carried out after collection of all the SIMS data, owing to the more destructive nature of the ICP-MS technique.

7.1. Supracrustal rocks

Four analyses were made of magmatic domains, one from banded amphibolite LS0417-1 and three from gneissic amphibolite LS0417-3 (Table 5). They show a small range in $\epsilon\text{Hf}(T)$ (where T is the weighted mean $^{207}\text{Pb}/^{206}\text{Pb}$ age of the domain) from +1.6 to +3.7 (Fig. 9) and a

Table 3
SHRIMP U–Pb data for zircons from Archean rocks in the Lushan area.

Spot	% ²⁰⁶ Pb _C	ppm U	ppm Th	²³² Th/ ²³⁸ U	ppm ²⁰⁶ Pb*	²⁰⁷ Pb*/ ²⁰⁶ Pb*	±%	²⁰⁷ Pb*/ ²³⁵ U	±%	²⁰⁶ Pb*/ ²³⁸ U	±%	err corr	²⁰⁶ Pb*/ ²³⁸ U Age	²⁰⁷ Pb*/ ²⁰⁶ Pb* Age	% Discordant
<i>Banded amphibolite (LS0417-1)</i>															
1.1Me-I	0.05	177	69	0.40	79.1	0.195	0.80	13.97	3.0	0.521	2.8	0.96	2702 ± 63	2781 ± 13	3
1.2Me-I	0.14	85	35	0.42	38.4	0.197	1.1	14.18	3.2	0.523	3.0	0.94	2712 ± 67	2798 ± 18	3
2.1Me-I	0.12	71	14	0.20	31.5	0.197	1.3	13.96	3.3	0.515	3.1	0.92	2678 ± 67	2798 ± 21	4
2.2Me-I	1.17	51	10	0.21	25.0	0.197	1.6	15.31	5.6	0.564	5.4	0.96	2885 ± 120	2799 ± 27	-3
3.1Me-I	0.14	48	9	0.19	22.1	0.197	1.5	14.39	3.7	0.531	3.4	0.91	2746 ± 75	2798 ± 25	2
4.1Me-II	0.03	237	6	0.03	103	0.182	2.0	12.72	3.5	0.507	2.9	0.82	2644 ± 63	2671 ± 33	1
4.2Me-I	0.29	55	14	0.26	23.3	0.196	1.6	13.23	3.7	0.490	3.3	0.90	2569 ± 70	2793 ± 26	8
5.1Me-III(?)	2.94	73	1	0.02	22.5	0.125	4.4	6.01	5.4	0.348	3.2	0.58	1926 ± 53	2032 ± 78	5
5.2Me-II	0.03	412	17	0.04	174	0.178	0.73	12.11	2.8	0.493	2.7	0.97	2584 ± 58	2635 ± 12	2
6.1Me-I	0.25	114	30	0.27	51.0	0.196	1.1	14.00	3.3	0.519	3.1	0.94	2695 ± 68	2790 ± 18	3
6.2Me-I	0.26	142	38	0.28	67.6	0.198	1.1	15.00	4.3	0.551	4.2	0.97	2827 ± 96	2806 ± 17	-1
7.1Me-II	0.15	212	12	0.06	97.1	0.180	0.77	13.18	2.9	0.533	2.8	0.96	2752 ± 63	2648 ± 13	-4
7.2Me-I	0.37	59	26	0.45	26.6	0.196	1.5	14.05	3.4	0.519	3.1	0.90	2696 ± 68	2796 ± 24	4
8.1Me-II	0.21	59	18	0.32	25.5	0.180	1.5	12.50	3.6	0.504	3.3	0.91	2629 ± 70	2654 ± 25	1
8.2Me-I	0.07	86	32	0.38	40.1	0.188	1.1	14.04	3.2	0.541	3.0	0.94	2788 ± 67	2726 ± 18	-2
9.1Me-II	0.15	127	4	0.03	54.7	0.182	1.9	12.59	3.4	0.502	2.9	0.84	2623 ± 62	2670 ± 31	2
9.2Mg	0.21	42	8	0.21	20.3	0.202	1.5	15.65	3.6	0.563	3.3	0.90	2879 ± 76	2840 ± 25	-1
9.3Me-II	0.35	167	7	0.05	69.0	0.183	1.1	12.11	5.4	0.480	5.3	0.98	2528 ± 110	2679 ± 18	6
10.1Me-I	0.11	46	18	0.40	20.2	0.194	1.5	13.55	5.2	0.507	5.0	0.96	2644 ± 110	2774 ± 25	5
10.2Me-II	0.05	106	8	0.08	44.7	0.179	1.0	12.09	3.1	0.489	2.9	0.94	2567 ± 62	2646 ± 17	3
11.1Mg	0.00	61	23	0.39	25.0	0.201	1.6	13.27	3.6	0.478	3.2	0.90	2519 ± 67	2836 ± 26	11
11.2Me-I	0.28	55	37	0.68	22.3	0.197	2.9	12.64	4.5	0.466	3.5	0.76	2467 ± 71	2799 ± 48	12
11.3Me-I	0.07	180	102	0.58	75.3	0.196	1.1	13.12	3.1	0.487	2.9	0.94	2556 ± 60	2789 ± 18	8
<i>Gneissic amphibolite (LS0417-3)</i>															
1.1Mg	0.24	40	93	2.40	19.0	0.199	1.9	15.16	3.8	0.552	3.3	0.87	2836 ± 76	2819 ± 31	-1
2.1Mg	0.39	57	64	1.14	29.0	0.202	1.5	16.32	4.2	0.585	3.9	0.94	2971 ± 93	2843 ± 24	-4
3.1Me-I	0.06	126	379	3.12	59.3	0.194	0.88	14.72	3.3	0.549	3.1	0.96	2822 ± 72	2779 ± 14	-2
4.1Me-II	0.36	101	82	0.84	46.3	0.181	1.3	13.31	3.2	0.533	3.0	0.92	2753 ± 66	2664 ± 21	-3
5.1Me-I	0.31	39	103	2.69	18.1	0.194	1.6	14.27	3.7	0.533	3.3	0.90	2755 ± 74	2778 ± 26	1
6.1Me-II	0.10	937	535	0.59	272	0.173	0.51	8.05	2.8	0.3380	2.7	0.98	1877 ± 44	2585 ± 9	27
7.1Me-II	0.15	372	265	0.74	144	0.181	0.76	11.21	2.9	0.450	2.8	0.96	2395 ± 56	2658 ± 13	10
8.1Me-I	0.95	35	21	0.62	16.0	0.189	2.2	13.81	4.3	0.530	3.6	0.85	2744 ± 81	2731 ± 37	0
9.1Me-I	0.44	37	99	2.80	17.1	0.195	1.9	14.60	3.9	0.542	3.4	0.88	2792 ± 77	2788 ± 31	0
10.1Me-II	0.15	226	208	0.95	83.2	0.178	0.79	10.48	2.9	0.427	2.8	0.96	2293 ± 54	2633 ± 13	13
11.1Me-I	0.20	49	58	1.22	22.3	0.194	1.6	14.21	3.6	0.532	3.2	0.89	2748 ± 72	2775 ± 27	1
12.1Mg	0.60	106	157	1.52	54.2	0.203	0.95	16.53	5.1	0.590	5.0	0.98	2988 ± 120	2853 ± 15	-5
<i>Gneissic biotite tonalite (LS0417-2)</i>															
1.1Mg	0.17	129	54	0.43	59.4	0.202	1.8	14.88	6.4	0.536	6.1	0.96	2765 ± 140	2839 ± 30	3
2.1Me-I	0.98	48	180	3.92	21.8	0.176	2.3	12.80	4.0	0.527	3.3	0.82	2731 ± 73	2615 ± 38	-4
2.2Mg	0.15	268	180	0.69	124	0.191	0.67	14.10	2.9	0.537	2.8	0.97	2771 ± 63	2746 ± 11	-1
3.1Me-I	0.29	20	57	2.92	9.77	0.190	2.6	14.83	4.8	0.566	4.1	0.84	2893 ± 95	2742 ± 43	-6
3.2Mg	0.14	102	31	0.31	48.7	0.198	1.1	15.09	3.1	0.553	2.9	0.94	2839 ± 67	2808 ± 17	-1
4.1Me-I	0.17	90	53	0.61	40.4	0.193	1.3	13.87	3.3	0.520	3.0	0.92	2701 ± 66	2770 ± 21	2
4.2Mg	0.09	193	105	0.56	88.9	0.190	0.90	14.02	3.0	0.536	2.8	0.95	2769 ± 64	2738 ± 15	-1
5.1Mg	0.05	78	29	0.39	36.6	0.205	1.1	15.43	3.2	0.546	3.0	0.94	2809 ± 68	2866 ± 18	2
6.1Me-I	0.35	49	89	1.85	24.6	0.197	1.5	15.64	3.6	0.577	3.3	0.91	2938 ± 78	2798 ± 24	-5
7.1Me-I	0.10	39	24	0.65	17.1	0.183	1.7	12.93	3.8	0.513	3.4	0.90	2671 ± 74	2677 ± 28	0
7.2Mg	0.10	138	50	0.38	63.5	0.198	0.87	14.65	3.0	0.535	2.9	0.96	2764 ± 65	2813 ± 14	2
8.1Mg	0.17	77	30	0.40	36.0	0.198	1.2	14.76	3.3	0.541	3.1	0.94	2786 ± 69	2810 ± 19	1
9.1Me-I	0.28	22	84	3.98	10.3	0.193	2.2	14.52	4.2	0.547	3.6	0.86	2813 ± 82	2763 ± 35	-2
10.1Mg	0.18	131	22	0.18	61.8	0.201	0.82	15.14	3.0	0.548	2.9	0.96	2815 ± 67	2830 ± 13	1
11.1Me-I	0.62	32	39	1.24	15.3	0.190	2.2	14.30	4.1	0.545	3.5	0.85	2803 ± 80	2745 ± 36	-2
12.1Me-I	0.47	27	188	7.07	12.5	0.194	2.5	14.07	6.4	0.527	5.9	0.92	2727 ± 130	2774 ± 41	2
13.1Me-I	0.94	34	50	1.49	15.6	0.199	2.4	14.23	4.3	0.520	3.6	0.83	2698 ± 78	2814 ± 40	4
14.1Me-I	0.78	24	112	4.81	11.3	0.190	2.5	14.11	4.5	0.540	3.7	0.83	2782 ± 83	2739 ± 41	-2
15.1Me-I	1.34	20	96	4.88	9.37	0.190	4.4	13.72	5.9	0.524	4.0	0.67	2717 ± 88	2740 ± 72	1
15.2Mg	0.21	666	193	0.30	253	0.193	1.4	11.75	3.1	0.442	2.7	0.89	2358 ± 54	2768 ± 23	15
16.1Mg	0.50	35	33	0.97	16.8	0.208	1.9	15.96	4.1	0.557	3.6	0.89	2854 ± 83	2888 ± 31	1
17.1Mg	0.39	69	35	0.52	31.1	0.200	1.4	14.51	3.5	0.526	3.2	0.91	2723 ± 70	2828 ± 24	4
18.1Mg	0.12	182	75	0.43	79.5	0.188	0.83	13.19	3.0	0.508	2.9	0.96	2647 ± 62	2728 ± 14	3
19.1Mg	0.17	51	28	0.57	24.1	0.202	1.8	15.36	3.7	0.551	3.2	0.87	2829 ± 74	2843 ± 30	0
20.1Mg	0.09	99	89	0.93	50.6	0.216	0.95	17.76	3.1	0.597	3.0	0.95	3019 ± 71	2949 ± 15	-2
<i>Gneissic hornblende–biotite tonalite (LS0417-4)</i>															
1.1Me-I	0.09	241	47	0.20	113	0.197	0.86	14.82	2.9	0.545	2.8	0.96	2806 ± 64	2802 ± 14	0
1.2Mg	0.41	51	39	0.78	25.6	0.201	1.4	16.00	3.9	0.578	3.7	0.94	2942 ± 87	2831 ± 23	-4
2.1Me-II	0.75	25	2	0.08	10.6	0.178	3.9	12.15	5.3	0.496	3.6	0.68	2598 ± 77	2631 ± 65	1
2.2Mg	0.17	65	36	0.58	30.8	0.202	1.3	15.39	3.3	0.553	3.1	0.92	2837 ± 71	2841 ± 21	0
4-2.3Mg	0.41	89	68	0.78	41.0	0.200	1.1	14.68	5.0	0.532	4.9	0.98	2750 ± 110	2827 ± 18	3
3.1Me-I	0.14	105	524	5.15	49.2	0.193	0.99	14.47	3.1	0.544	2.9	0.95	2802 ± 66	2767 ± 16	-1
3.2Me-I	0.46	40	58	1.48	18.1	0.190	1.7	13.67	3.8	0.522	3.4	0.90	2709 ± 76	2740 ± 28	1

Table 3 (continued)

Spot	% ²⁰⁶ Pb _c	ppm U	ppm Th	²³² Th/ ²³⁸ U	ppm ²⁰⁶ Pb*	²⁰⁷ Pb*/ ²⁰⁶ Pb*	±%	²⁰⁷ Pb*/ ²³⁸ U	±%	²⁰⁶ Pb*/ ²³⁸ U	±%	err corr	²⁰⁶ Pb*/ ²³⁸ U Age	²⁰⁷ Pb*/ ²⁰⁶ Pb* Age	% Discordant
<i>Gneissic hornblende–biotite tonalite (LS0417–4)</i>															
4.1Me-II	0.27	23	12	0.52	9.45	0.177	2.5	11.61	4.6	0.476	3.9	0.84	2508 ± 81	2626 ± 42	4
4.2Mg	0.18	73	38	0.53	35.2	0.199	1.1	15.26	3.2	0.557	3.0	0.94	2855 ± 69	2814 ± 18	–1
5.1Mg	0.50	74	39	0.55	33.7	0.203	1.4	14.81	3.4	0.529	3.1	0.91	2737 ± 69	2851 ± 23	4
5.2Mg	0.00	66	74	1.16	30.6	0.205	1.2	15.27	3.2	0.539	3.0	0.93	2781 ± 68	2868 ± 19	3
6.1Me-I	0.04	438	189	0.44	187	0.201	0.48	13.73	2.8	0.496	2.7	0.98	2598 ± 59	2831 ± 8	8
6.2Mg	0.00	81	77	0.98	39.8	0.202	1.0	15.97	3.1	0.573	3.0	0.95	2920 ± 69	2844 ± 16	–3
7.1Mg	0.08	73	46	0.65	34.9	0.212	1.1	16.31	3.2	0.557	3.0	0.94	2855 ± 69	2923 ± 17	2
7.2Mg	0.88	95	51	0.55	44.0	0.196	1.8	14.43	5.2	0.533	4.9	0.94	2754 ± 110	2796 ± 29	1
8.1Me-II	1.79	18	10	0.55	7.74	0.183	4.1	12.25	5.7	0.486	3.9	0.68	2555 ± 81	2677 ± 68	5
9.1Me-I	0.72	18	11	0.65	8.45	0.194	3.7	14.39	5.6	0.538	4.1	0.74	2775 ± 94	2776 ± 62	0
9.2Mg	0.14	90	77	0.89	42.2	0.190	1.6	14.33	3.8	0.547	3.4	0.90	2812 ± 79	2812 ± 27	–3
10.1Mg	0.20	56	54	0.98	27.9	0.199	1.4	15.80	3.4	0.575	3.1	0.91	2928 ± 74	2821 ± 23	–4
10.2Me-I	0.04	272	137	0.52	121	0.191	1.5	13.66	3.2	0.519	2.8	0.88	2694 ± 61	2750 ± 25	2
11.1Me-I	0.28	22	13	0.63	10.3	0.193	2.2	14.40	4.4	0.542	3.8	0.86	2793 ± 86	2765 ± 37	–1
11.2Mg	0.45	61	62	1.04	30.9	0.203	1.5	16.46	3.6	0.588	3.3	0.91	2980 ± 78	2852 ± 25	–4
12.1Me-I	0.38	91	26	0.29	39.9	0.188	1.3	13.22	4.8	0.509	4.7	0.96	2654 ± 100	2726 ± 22	3
12.2Mg	0.20	70	56	0.82	34.1	0.211	2.9	16.37	5.0	0.563	4.1	0.82	2877 ± 95	2913 ± 46	1
13.1Mg	0.35	69	47	0.71	32.5	0.204	1.3	15.26	3.3	0.543	3.1	0.92	2797 ± 70	2856 ± 21	2
13.2Mg	0.27	101	87	0.89	47.5	0.197	1.1	14.78	3.1	0.545	2.9	0.94	2805 ± 67	2798 ± 18	0
14.1Mg	0.52	46	12	0.28	19.3	0.181	2.0	12.15	3.8	0.487	3.2	0.86	2556 ± 69	2663 ± 32	4
14.2Me-I	0.72	34	6	0.19	16.4	0.194	2.1	14.81	4.0	0.554	3.5	0.85	2843 ± 79	2774 ± 34	–3
15.1Me-I	1.05	543	138	0.26	224	0.190	0.89	12.40	2.9	0.473	2.7	0.95	2497 ± 56	2743 ± 15	9
16.1Me-I	0.06	465	36	0.08	191	0.195	0.56	12.89	3.0	0.479	3.0	0.98	2523 ± 63	2786 ± 9	9
16.2Mg	0.34	63	49	0.81	29.8	0.201	1.4	15.20	3.5	0.550	3.2	0.92	2823 ± 73	2831 ± 23	0
17.1Mg	0.09	604	127	0.22	266	0.199	1.0	14.05	2.9	0.512	2.7	0.94	2667 ± 60	2817 ± 17	5

Errors are 1-sigma and Pb* indicates the radiogenic portions.

Data were ²⁰⁴Pb corrected, using measured values.

% discordance = % discordance defined as $[(^{206}\text{Pb}/^{238}\text{U})_{\text{age}} / (^{207}\text{Pb}/^{206}\text{Pb})] \times 100$.

Note: Mg means magmatic zircons, Me-I, Me-II and Me-III represent zircons formed during the first, second and third metamorphic events, respectively.

restricted range in $T_{\text{DM}}(\text{Hf})$ model age from 2968 to 3046 Ma, indicating derivation from a depleted mantle source only a short time prior to crystallization. Fifteen analyses of metamorphic domain Me-I on zircons from LS0417-1 range in $\epsilon\text{Hf}_{\text{T}}$ from –1.2 to +4.3 and in $T_{\text{DM}}(\text{Hf})$ model age from 2898 to 3104. This is only slightly greater than for the magmatic domains and indicates that the first high-grade metamorphic event at ~2780 Ma had little to no effect on the Lu–Hf system. Three analyses made on Me-II domains in zircons from LS0417-1 range in $\epsilon\text{Hf}_{\text{T}}$ from –1.6 to +1.2 and in $T_{\text{DM}}(\text{Hf})$ model age from 2894 to 2997, likewise indicating that metamorphism at ~2650 Ma had no effect on the Lu–Hf systematics (Fig. 9). However, the one analysis obtained from the rare Me-III domains has an $\epsilon\text{Hf}_{\text{T}}$ of –11.8 and $T_{\text{DM}}(\text{Hf})$ model age of 2854 Ma. Unfortunately, no oxygen data were collected on Me-III sites, so it remains tantalizing as to the potentially greater effect of the ~2030 Ma metamorphic event on the zircon isotopic system.

7.2. Tonalites

A total of 13 analyses were made on magmatic domains in gneissic biotite tonalite sample LS0417-2 and 15 from gneissic hornblende–biotite tonalite sample LS0417-4 (Table 5). They show a range in $\epsilon\text{Hf}_{\text{T}}$ from –3.3 to +8.9, although the majority lies between –0.8 and +5.0, which is essentially similar to that observed in the amphibolitic zircons. There is no obvious explanation of the more extreme values of –3.3 and +8.9 from two sites; unfortunately, the destructive nature of the ICP-MS technique meant that these sites could not be re-evaluated. The $T_{\text{DM}}(\text{Hf})$ model ages for the tonalite magmatic zircon domains range from 2759 to 3229 Ma, which is slightly greater than for the amphibolite zircons but not substantially different (Fig. 9), since the two extreme values were obtained from the sites that also yielded the extreme $\epsilon\text{Hf}_{\text{T}}$ values. Overall, they suggest extraction from a depleted mantle source of similar age to that from which the amphibolites were generated. A total of 13 analyses were made on Me-I domains from both samples and these reveal a range in $\epsilon\text{Hf}_{\text{T}}$ from –2.5 to +4.2 and in $T_{\text{DM}}(\text{Hf})$ model age from 2844 to 3023 Ma (Table 5). These values are virtually identical to the results obtained from Me-I domains in the

amphibolite zircons and indicate no effect of high-grade metamorphism at ~2770 Ma. Only one Me-II domain was analyzed (LS0417-4, spot 2.1Me-II) and this records an $\epsilon\text{Hf}_{\text{T}}$ value of –1.5 and $T_{\text{DM}}(\text{Hf})$ model age of 2984 (Table 5), showing no difference to similar domains in the amphibolite zircons and no effect of high-grade metamorphism at ~2640 Ma.

8. Discussion

Ages obtained in this study are summarized in Table 6. The magmatic zircons from amphibolite samples LS0417-1 and LS0417-3 have weighted mean ²⁰⁷Pb/²⁰⁶Pb ages of 2838 ± 35 Ma and 2845 ± 23 Ma, respectively. Likewise, the magmatic zircons from tonalite samples LS0417-2 and LS0417-4 have ages of 2829 ± 18 Ma and 2832 ± 11 Ma, which are identical within error. If the uncertainties are excluded, it could be argued that the tonalites are just slightly younger, in harmony with the field evidence. These data not only confirm the Mesoproterozoic age of tonalitic magmatism at Lushan (Kröner et al., 1988) but also that there was an episode of coeval Mesoproterozoic volcanism that resulted in mafic lavas being intercalated with other supracrustal rocks, including khondalite protoliths, that now form rafts and enclaves within the tonalites. Lushan is the only area currently known in the Trans-North China Orogen where Mesoproterozoic rocks are present over a significant area; unlike in the Hengshan and Fuping complexes farther to the north (Fig. 1a) where rare individual lenses and layers in banded gneisses record slightly younger ages of ~2.7 Ga (Kröner et al., 2005, 2006).

Most magmatic zircons from the four samples have similar Hf isotope compositions (Fig. 9). Excluding the ‘outlier’ analyses LS0417-2-20 Mg and LS0417-4-14 Mg (the former having the lowest $\epsilon\text{Hf}_{\text{T}}$ value and the oldest $T_{\text{DM}}(\text{Hf})$ model age; the latter having the highest $\epsilon\text{Hf}_{\text{T}}$ value and lowest $T_{\text{DM}}(\text{Hf})$ model age – Table 5), the $T_{\text{DM}}(\text{Hf})$ values range from 2903 to 3123, with an average $T_{\text{DM}}(\text{Hf})$ of 2995 Ma, only slightly older than the zircon U–Pb ages. Again, excluding the two ‘outliers’, their $\epsilon\text{Hf}_{\text{T}}$ ranges from –0.8 to +5.0 (average of +2.5), with the weakly positive values suggesting that they were mainly derived

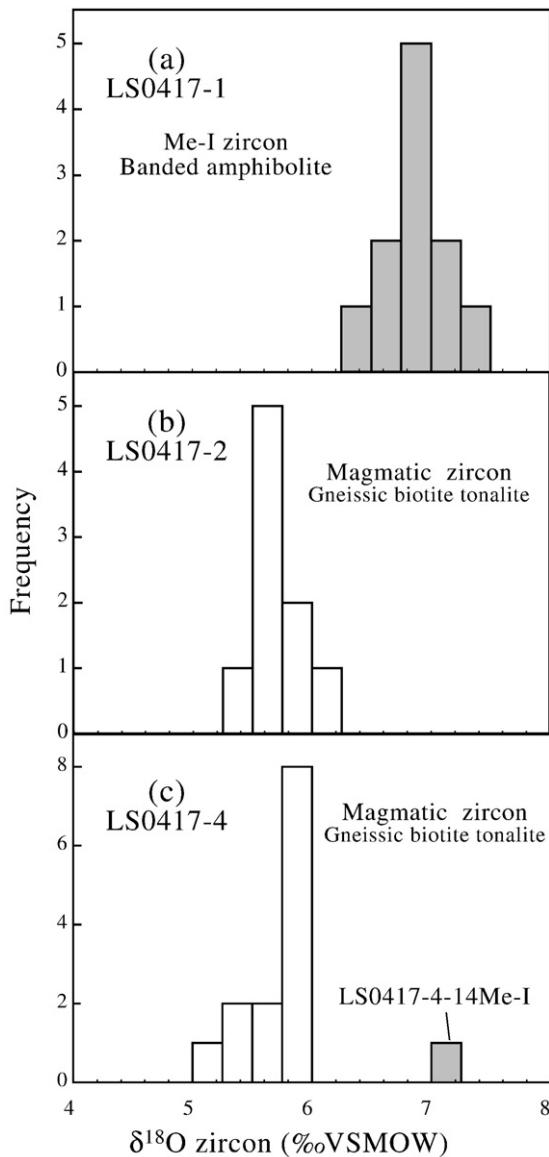


Fig. 8. Values of $\delta^{18}\text{O}$ for zircons from Archean rocks in the Lushan area. (a) Banded amphibolite (LS0417-1); (b) Gneissic biotite tonalite (LS0417-2); (c) Gneissic hornblende–biotite tonalite (LS0417-4).

from a depleted mantle source. The few weakly negative values may indicate some contribution from older continental material, or else that they were derived from a juvenile continental source with a very short crustal residence time.

Our new, precise, multi-isotope zircon study reveals that the amphibolites and tonalites at Lushan subsequently underwent a common history, recording two subsequent periods of metamorphism and indicating that they must have been interleaved at a very early stage in their geological history. All four samples in this study record a metamorphic event (Me-I) between 2.79 and 2.77 Ga (Table 6). The metamorphic zircons have higher $\delta^{18}\text{O}$ values (6.5 to 7.3‰) than the magmatic zircons (5.1 to 5.9‰), indicating the ingress of crustal fluids during metamorphic reconstitution of the zircon. This metamorphism took place under upper amphibolite facies conditions based on: 1) many of these zircons show fir-tree and sector zoning, which are commonly observed in high-grade metamorphic zircons (Vavra et al., 1996), 2) some zircons contain clinopyroxene inclusions in these domains, providing direct evidence for their formation under relatively high-grade metamorphic conditions, and 3) tonalite sample LS0417-2 is extensively cut by

anatectic veins (Fig. 2b) indicating partial melting and the availability of fluid. This is the first time that such features have been recorded from this part of the Trans-North China Orogen and the first time that a tectonothermal event of this age has been recognized in the NCC.

The Me-I zircon domains commonly have Th/U ratios greater than 0.1. This has previously been recorded from zircons from high-grade metamorphic rocks, especially ultra-high temperature ones (Zhou et al., 2004; Wan et al., 2006a; Santosh et al., 2007). However, some of these Me-I domains have extremely high Th/U ratios, with the highest being 7.1 (Table 3). These zircons are generally low in U (commonly <40 ppm), but some with relatively high U contents are also present (105 ppm, LS0417-4-3.1Me-I). It is possible that Th is present in excess amounts, either due to retention in the crystal lattice during high-

Table 4

Oxygen isotopic compositions of zircons from Archean rocks in the Lushan area (G989) and zircon standard 91500 measured in situ by ion microprobe.

An.#	Sample#-Zrc#-O isotope spot#	U-Pb dating spot #	Hf isotope spot #	$d^{18}\text{O}$ 2 SD		
				Raw	VSMOW	
1	G989 91500			11.95		
2	G989 91500			11.97		
3	G989 91500			11.96		
4	G989 91500			11.86		
5	G989 91500			11.89		
6	G989 91500			11.79		
	Average (#1–6)			11.90	0.14	
7	G989 LS0417-1-7Me-I	7.2Me-I	01Me-I	9.44	7.3	0.28
8	G989 LS0417-1-8Me-I	8.2Me-I	02Me-I	9.16	7.0	0.28
9	G989 LS0417-1-9Mg	9.2Mg	09Mg	9.16	7.0	0.28
10	G989 LS0417-1-10Me-I	10.1Me-I	11Me-I	8.99	6.9	0.28
11	G989 LS0417-1-4Me-II	4.1Me-II	13Me-II	9.10	7.0	0.28
12	G989 LS0417-1-5aMe-II	5.2Me-II	15Me-II	8.59	6.4	0.28
13	G989 LS0417-1-5bMe-II	5.2Me-II	15Me-II	8.67	6.5	0.28
14	G989 LS0417-1-3Me-I	3.1Me-I	16Me-I	8.92	6.8	0.28
15	G989 LS0417-1-1Me-I			8.86	6.7	0.28
16	G989 LS0417-1-2Me-I	2.1Me-I	20Me-I	8.94	6.8	0.28
	Average (#7–16)			8.94	6.8	0.50
17	G989 LS0417-4-2Mg	2.2Mg	02Mg	7.92	5.8	0.28
18	G989 LS0417-4-1Mg	1.2Mg		8.03	5.9	0.28
19	G989 LS0417-4-4Mg	4.2Mg	07Mg	7.86	5.7	0.28
20	G989 LS0417-4-3Mg			7.98	5.8	0.28
21	G989 LS0417-4-6Mg	6.2Mg	13Mg	7.95	5.8	0.28
	Average (#17–21)			7.95	5.8	0.13
22	G989 91500			12.11		
23	G989 91500			12.17		
24	G989 91500			12.22		
25	G989 91500			12.11		
	Average (#22–25)			12.15	0.11	
	Average (#1–6, 22–25)			12.00	0.28	
26	G989 LS0417-4-7Mg	7.1Mg	10Mg	8.05	5.8	0.31
27	G989 LS0417-4-9Mg	9.2Mg	16Mg	7.36	5.1	0.31
28	G989 LS0417-4-10Mg	10.1Mg	15Mg	8.15	5.9	0.31
29	G989 LS0417-4-12Mg	12.2Mg	14Mg	7.68	5.5	0.31
30	G989 LS0417-4-11Mg	11.2Mg	17Mg	7.55	5.3	0.31
31	G989 LS0417-4-14Me-I	14.2Me-I	19Me-I	9.24	7.0	0.31
32	G989 LS0417-4-16Mg	16.2Mg	21Mg	7.96	5.7	0.31
	average (#26–32, excluding 14Me-I)			8.05	5.6	1.23
33	G989 LS0417-2-2 Ma	2.2Mg	01Mg (or 02Mg)	8.26	6.0	0.31
34	G989 LS0417-2-8 Ma	8.1Mg	09 Ma	7.58	5.4	0.31
35	G989 LS0417-2-9 Ma			7.90	5.7	0.31
36	G989 LS0417-2-6 Ma			8.13	5.9	0.31
37	G989 LS0417-2-13 Ma			8.05	5.8	0.31
38	G989 LS0417-2-20 Ma	20.1Mg	17Mg	7.75	5.5	0.31
39	G989 LS0417-2-19 Ma	19.1Mg	18Mg	7.83	5.6	0.31
40	G989 LS0417-2-16 Ma	16.1Mg	20Mg	7.79	5.6	0.31
	average (#33–40)			7.83	5.7	0.44
41	G989 91500			12.09		
42	G989 91500			12.25		
43	G989 91500			11.94		
44	G989 91500			11.77		
	Average (#41–44)			12.01	0.41	
	Average (#22–25, 41–44)			12.08	0.31	

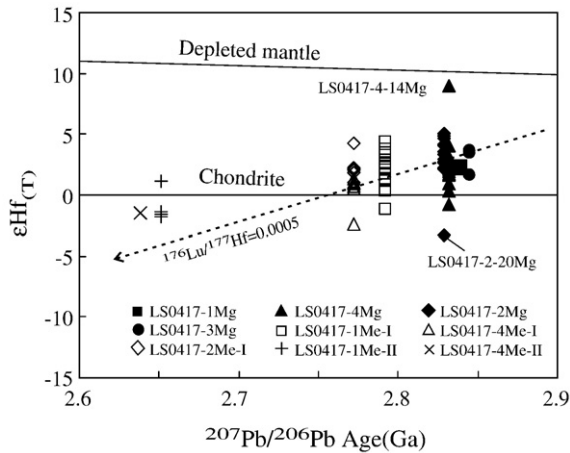


Fig. 9. $\epsilon\text{Hf}_{(T)}$ vs. $^{207}\text{Pb}/^{206}\text{Pb}$ age diagram for zircon data from Archean rocks in the Lushan area. The $^{176}\text{Lu}/^{177}\text{Hf}$ reference line shown is based on the average model age for the data.

grade metamorphism or, more likely, because there were Th-rich mineral inclusions in these domains, since they are known to be inclusion-rich as discussed above. Unfortunately, we could not re-check this because all the sites with high Th/U ratio were destroyed during LA-ICP-MS Hf analysis. However, the fact that gneissic biotite-rich tonalite (LS0417-2) is cut by anatectic veins (Fig. 2b) indicates that a fluid was available during metamorphism and it is likely that this resulted in the 'igneous-like' Th/U ratios in some grains (see Grant et al., this issue).

The $\epsilon\text{Hf}_{(T)}$ of zircons from these early metamorphic (Me-I) domains in banded amphibolite sample LS0417-1 range from -1.2 to $+4.3$ (average of $+1.8$) and their T_{DM} (Hf) model ages from 2898 to 3104 Ma (average of 2991 Ma). Both tonalite samples LS0417-2 and LS0417-4 record the same age for Me-I domains, with their $\epsilon\text{Hf}_{(T)}$ ranging from -2.5 to $+4.2$ (average of $+1.3$) and their T_{DM} (Hf) and 2884 to 3023 Ma (average of 2984 Ma). All the Me-I zircon domains are thus similar in Hf isotope composition to the magmatic zircons, indicating that the Lu–Hf isotopic system was unaffected by the metamorphic event.

The Me-II zircon domains formed during the second metamorphic event reveal a range in Th/U from 0.03 to 0.95, less extreme than for Me-I domains. Only 3 analyses for oxygen were made (all from sample LS0417-1) and these show a similar elevation in value to Me-I domains, with values ranging from 6.4 to 7.0‰. Likewise, only limited Hf analyses (4) were made of these domains and, within this constraint, they show no significant variation in either their $\epsilon\text{Hf}_{(T)}$ values (-1.6 to $+1.2$) or their T_{DM} (Hf) model ages (2894 to 2997), indicating that their was no disturbance of the Hf isotope system at ~ 2.65 Ga (Fig. 8).

The recognition of a third generation of metamorphic domain (Me-III) in zircon 5.1 from banded amphibolite LS0417-1, with a rather imprecise age of 2032 ± 78 Ma (Table 2), is intriguing, especially when its $\epsilon\text{Hf}_{(T)}$ of -11.8 is the lowest recorded during this study. Unfortunately, insufficient data are available to evaluate this further, but it is worthy of further investigation.

It is difficult to evaluate the significance of these new results within the context of the evolution of the North China Craton. Firstly, no rocks as old as 2.82 Ga have previously been recorded from the Trans-North China Orogen outside of the Lushan area (Kröner et al., 1988; this study). Similarly, there is no previous record of metamorphic events at 2.77–2.79 Ga or at 2.64–2.67 Ga within the NCC. One feature that does emerge is the close temporal association of magmatism with the first high-grade metamorphic event. This is a feature recorded at a later time in the NCC, between 2.53 and 2.50 Ga, where TTG magmatism was followed shortly after by upper amphibolite to granulite facies metamorphism. For this situation, the distribution across large tracts of the NCC of mafic granulites with

counter-clockwise P/T/t paths and metamorphic ages of 2.5 Ga (Zhao et al., 1998, 1999) has led to the suggestion that metamorphism may be a reflection of basaltic underplating, possible due to mantle plume activity (see also Yang et al., 2008; Grant et al., this issue). Whilst it is clearly premature to draw such conclusions for the events between 2.82 and 2.79 Ga at Lushan, these new results provide impetus for further work in the southern part of the Trans-North China Orogen in order to resolve this issue.

Finally, it may be significant that the high-grade meta-igneous rocks at Lushan show no evidence of subsequent metamorphism at ~ 1.85 Ga, as is ubiquitous in the northern and central parts of the Trans-North China Orogen (see Zhao et al., 2005 for a recent review). Indeed, this is quite unexpected, since graphite–garnet–sillimanite and garnet-bearing granitoid gneiss from the Shangtaihua 'group' at Lushan both record this event (Wan et al., 2006b). It may be that the geology of the Lushan area is more complex than appears from published maps (Yang et al., 2008), with much tectonic interleaving of rocks of diverse age. Whilst we can add no further information to this debate based on the current data, our findings are important and it becomes imperative to re-examine in detail all the supracrustal and TTG occurrences near the southern margin of the NCC.

9. Conclusions

By the application of multi-isotope techniques we have been able to characterise complex zircons from meta-igneous rocks at Lushan in the southern part of the Trans-North China Orogen and, in the process, identify two events not previously recognized in the NCC. At Lushan (Fig. 1), supracrustal amphibolites were intercalated with khondalitic metasediments and both were subsequently entrained in tonalites as rafts from a few centimetres to kilometres in length. SIMS (SHRIMP II) U–Pb data establish that the amphibolites and tonalites are coeval, with magmatic crystallization ages of 2838 ± 35 Ma and 2845 ± 23 Ma (amphibolite samples LS0417-1 and LS0417-3) and 2829 ± 18 Ma and 2832 ± 11 Ma (meta-tonalite samples LS0417-2 and LS0417-4), respectively. Magmatic zircon domains, characterized by oscillatory zoning in CL images, have mantle $\delta^{18}\text{O}$ values of 5.1 to 5.9‰, as obtained by SIMS (CAMECA ims 1280) analysis. This is confirmed by multicollector ICP-MS Lu–Hf analysis of magmatic domains, which indicates derivation from a depleted mantle source ($\epsilon\text{Hf}_{(T)}$ -0.8 to $+5.0$), with some minor crustal contamination, at 2995 Ma (average of all samples).

An early generation of metamorphic domain (Me-I) is consistently developed in zircons from all four samples studied. It is characterized by weak sector and fir-tree zoning and records a similar U–Pb age in amphibolite and meta-tonalite, ranging from 2776 ± 20 Ma to 2792 ± 11 Ma for the amphibolites and occurring at $2772 \pm 22/17$ Ma in the tonalites, indistinguishable within error. The presence of abundant mineral inclusions, including clinopyroxene, in amphibolite sample LS0417-1 (Fig. 5) confirms the metamorphic origin of these domains and supports the view that it records growth of new zircon in the presence of a fluid, generated during high-grade regional metamorphism that locally resulted in anatexis of the tonalites (Fig. 2b). Likewise, the $\delta^{18}\text{O}$ data support interaction with crustal fluids, since values range from 6.4 to 7.3‰, being consistently higher than the magmatic domains. There is no disturbance to the Lu–Hf system and the $\epsilon\text{Hf}_{(T)}$ and T_{DM} (Hf) model ages are identical to those determined for magmatic zircon. A metamorphic event at this age has not previously been recorded in the NCC.

An outer metamorphic domain (Me-II) is recognized in zircon CL images of three of the four samples analyzed (excluding biotite-rich tonalite sample LS0417-2). It characteristically forms narrow rims that are dark in CL and records ages of 2651 ± 13 Ma and 2671 ± 25 Ma in the amphibolites and 2638 ± 61 Ma in hornblende tonalite sample LS0417-4, indistinguishable within the albeit fairly large errors. Only limited oxygen isotope data were collected from these rims, but they show a

Table 5
Hf isotope compositions of zircons from Archean rocks in the Lushan area.

No.	Spot no.	t (Ma)	$^{176}\text{Yb}/^{177}\text{Hf}$	$^{176}\text{Lu}/^{177}\text{Hf}$	$^{176}\text{Hf}/^{177}\text{Hf}(c)$	$2s_m$	$\varepsilon\text{Hf}(0)$	$\varepsilon\text{Hf}(T)$	2 s	$T_{DM}(\text{Hf})$	$f_{Lu/Hf}$
<i>Banded amphibolite (LS0417-1)</i>											
09Mg	9.2Mg	2838	0.0137	0.0004	0.281055	0.000019	-60.7	2.3	0.7	3012	-0.99
01Me-I	7.2Me-I	2792	0.0292	0.0009	0.281116	0.000024	-58.6	2.6	0.9	2966	-0.97
02Me-I	8.2Me-I	2792	0.0105	0.0004	0.281138	0.000027	-57.8	4.3	1.0	2898	-0.99
03Me-I	Me-I	2792	0.0166	0.0005	0.281058	0.000025	-60.6	1.1	0.9	3017	-0.98
04Me-I	Me-I	2792	0.0095	0.0003	0.281106	0.000019	-58.9	3.2	0.7	2937	-0.99
06Me-I	Me-I	2792	0.0115	0.0003	0.281025	0.000017	-61.8	0.3	0.6	3047	-0.99
07Me-I	Me-I	2792	0.0220	0.0009	0.281147	0.000020	-57.5	3.7	0.7	2922	-0.97
08Me-I	Me-I	2792	0.0118	0.0003	0.281027	0.000022	-61.7	0.4	0.8	3043	-0.99
10Me-I	Me-I	2792	0.0153	0.0005	0.281057	0.000019	-60.7	1.2	0.7	3013	-0.99
11Me-I	10.1Me-I	2792	0.0146	0.0005	0.281096	0.000018	-59.3	2.6	0.7	2962	-0.99
12Me-I	4.2Me-I	2792	0.0157	0.0005	0.281082	0.000017	-59.8	2.0	0.6	2983	-0.98
16Me-I	3.1Me-I	2792	0.0175	0.0005	0.281074	0.000019	-60.1	1.7	0.7	2995	-0.98
17Me-I	1.1Me-I	2792	0.0234	0.0007	0.281099	0.000021	-59.2	2.3	0.7	2976	-0.98
18Me-I	1.2Me-I	2651	0.0073	0.0002	0.281049	0.000021	-60.9	1.5	0.8	3006	-0.99
19Me-I	Me-I	2792	0.0144	0.0004	0.281052	0.000021	-60.8	1.2	0.8	3014	-0.99
20Me-I	2.1Me-I	2792	0.0141	0.0005	0.280988	0.000020	-63.1	-1.2	0.7	3104	-0.99
05Me-II	Me-II	2651	0.0131	0.0004	0.281070	0.000019	-60.2	-1.5	0.7	2993	-0.99
13Me-II	4.1Me-II	2651	0.0100	0.0003	0.281061	0.000024	-60.5	-1.6	0.9	2997	-0.99
15Me-II	5.2Me-II	2651	0.0089	0.0003	0.281137	0.000019	-57.8	1.2	0.7	2894	-0.99
14Me-III(?)	5.1Me-III(?)	2032	0.0121	0.0004	0.281172	0.000020	-56.6	-11.8	0.7	2854	-0.99
<i>Gneissic amphibolite (LS0417-3)</i>											
01Mg	Mg	2845	0.0177	0.0004	0.281030	0.000020	-61.6	1.6	0.7	3046	-0.99
02Mg	Mg	2845	0.0093	0.0002	0.281072	0.000019	-60.14	3.4	0.7	2976	-0.99
03Mg	Mg	2845	0.0163	0.0004	0.281086	0.000018	-59.6	3.7	0.7	2968	-0.99
<i>Gneissic biotite tonalite (LS0417-2)</i>											
01Mg	2.2Mg	2829	0.0127	0.0003	0.281084	0.000019	-59.7	3.3	0.7	2966	-0.99
02Mg	Mg	2829	0.0087	0.0002	0.281128	0.000024	-58.2	5.0	0.9	2903	-0.99
03Mg	Mg	2829	0.0428	0.0011	0.281092	0.000021	-59.4	2.1	0.7	3015	-0.97
04Mg	Mg	2829	0.0708	0.0017	0.281164	0.000022	-56.9	3.5	0.8	2965	-0.95
05Mg	Mg	2829	0.0218	0.0005	0.281083	0.000018	-59.7	3.0	0.6	2981	-0.99
08Mg	4.2Mg	2829	0.0206	0.0006	0.281083	0.000025	-59.7	2.7	0.9	2990	-0.98
09Mg	8.1Mg	2829	0.0166	0.0004	0.281127	0.000025	-58.2	4.6	0.9	2918	-0.99
12Mg	7.2Mg	2829	0.0095	0.0003	0.281051	0.000020	-60.9	2.3	0.7	3006	-0.99
16Mg	Mg	2829	0.0206	0.0006	0.281121	0.000022	-58.4	4.1	0.8	2937	-0.98
17Mg	20.1Mg	2829	0.0243	0.0009	0.281094	0.000031	-59.3	2.6	1.1	2995	-0.97
18Mg	19.1Mg	2829	0.0125	0.0004	0.281133	0.000044	-58.0	4.9	1.6	2909	-0.99
19Mg	17.1Mg	2829	0.0235	0.0007	0.281124	0.000023	-58.3	4.0	0.8	2941	-0.98
20Mg	16.1Mg	2829	0.0438	0.0016	0.280968	0.000043	-63.8	-3.3	1.5	3229	-0.95
06Me-I	Me-I	2772	0.0170	0.0005	0.281087	0.000022	-59.6	1.8	0.8	2975	-0.99
07Me-I	4.1Me-I	2772	0.0128	0.0004	0.281091	0.000028	-59.5	2.2	1.0	2961	-0.99
10Me-I	9.1Me-I	2772	0.0109	0.0003	0.281089	0.000024	-59.5	2.3	0.9	2957	-0.99
11Me-I	6.1Me-I	2772	0.0229	0.0006	0.281067	0.000022	-60.3	1.0	0.8	3007	-0.98
13Me-I	11.1Me-I	2772	0.0123	0.0004	0.281150	0.000042	-57.4	4.2	1.5	2884	-0.99
14Me-I	12.1Me-I	2772	0.0166	0.0005	0.281094	0.000032	-59.3	2.0	1.2	2967	-0.98
15Me-I	13.1Me-I	2772	0.0112	0.0003	0.281078	0.000024	-59.9	1.8	0.8	2975	-0.99
<i>Gneissic hornblende-biotite tonalite (LS0417-4)</i>											
02Mg	2.2 Ma	2832	0.0246	0.0006	0.281027	0.000030	-61.7	0.9	1.1	3061	-0.98
03Mg	Ma	2832	0.0129	0.0003	0.281040	0.000030	-61.2	1.9	1.1	3021	-0.99
05Mg	5.1 Ma	2832	0.0075	0.0002	0.281030	0.000024	-61.6	1.7	0.9	3030	-0.99
06Mg	5.2 Ma	2832	0.0151	0.0003	0.281048	0.000026	-61.0	2.1	0.9	3014	-0.99
07Mg	4.2 Ma	2832	0.0105	0.0003	0.280995	0.000022	-62.9	0.3	0.8	3080	-0.99
10Mg	7.1 Ma	2832	0.0105	0.0003	0.281098	0.000024	-59.2	4.0	0.9	2942	-0.99
11Mg	Ma	2832	0.0090	0.0003	0.281050	0.000024	-60.9	2.3	0.9	3007	-0.99
13Mg	6.2 Ma	2832	0.0167	0.0004	0.281061	0.000023	-60.5	2.4	0.8	3004	-0.99
14Mg	12.2 Ma	2832	0.0065	0.0002	0.281233	0.000027	-54.4	8.9	1.0	2759	-0.99
15Mg	10.1 Ma	2832	0.0161	0.0004	0.281056	0.000021	-60.7	2.3	0.8	3008	-0.99
16Mg	9.2 Ma	2832	0.0125	0.0003	0.280966	0.000024	-63.9	-0.8	0.8	3123	-0.99
17Mg	11.2 Ma	2832	0.0143	0.0003	0.281034	0.000032	-61.5	1.6	1.1	3035	-0.99
18Mg	Ma	2832	0.0067	0.0002	0.281067	0.000023	-60.3	3.1	0.8	2978	-0.99
20Mg	14.1 Ma	2832	0.0151	0.0004	0.281067	0.000025	-60.3	2.6	0.9	2998	-0.99
21Mg	16.2 Ma	2832	0.0097	0.0003	0.281049	0.000023	-61.0	2.2	0.8	3011	-0.99
04Me-I	1.1Me-I	2772	0.0081	0.0002	0.281038	0.000021	-61.3	-2.5	0.8	3017	-0.99
08Me-I	3.2Me-I	2772	0.0138	0.0003	0.281054	0.000025	-60.8	1.0	0.9	3005	-0.99
09Me-I	3.1Me-I	2772	0.0206	0.0005	0.281063	0.000022	-60.5	0.9	0.8	3008	-0.99
12Me-I	6.1Me-I	2772	0.0099	0.0004	0.281067	0.000033	-60.3	1.3	1.2	2995	-0.99
19Me-I	14.2Me-I	2772	0.0108	0.0003	0.281048	0.000032	-61.0	0.7	1.1	3016	-0.99
22Me-I	16.1Me-I	2772	0.0077	0.0003	0.281039	0.000036	-61.3	0.5	1.3	3023	-0.99
01Me-II	2.1Me-II	2638	0.0118	0.0004	0.281076	0.000030	-60.0	-1.5	1.1	2984	-0.99

Table 6

Summary of zircon U–Pb data for Archean rocks in the Lushan area.

Sample no.	Rock type	Magmatic age (Ma)	Metamorphic age (Me-I)	Metamorphic age (Me-II)
LS0417-1	Amphibolite	2838 ± 35	2792 ± 12	2651 ± 13
LS0417-3	Amphibolite	2845 ± 23	2776 ± 20	2671 ± 25
LS0417-2	Gneissic tonalite	2829 ± 18	2772 ± 22	
LS0417-4	Gneissic tonalite	2832 ± 11	2772 ± 17	2638 ± 61

Note: Ages in Ma.

similar range in value (6.4 to 7.0‰) to the Me-I domains. Furthermore, the Lu–Hf system was undisturbed during this event. As with Me-I, there is no previous record of a metamorphic event at this time in the NCC.

A single light CL rim with weak zoning is developed around zircon grain 5 in amphibolite sample LS0417-1 (Fig. 4d). It records an age of 2032 ± 78 Ma and has the lowest $\epsilon_{\text{Hf}(T)}$ value obtained in this study (-11.8). It appears to record an early Paleoproterozoic event (Me-III?), but, since the data are so sparse, further speculation is unwarranted until further data can be obtained.

Since the rocks at Lushan are older (Kröner et al., 1988; this study) than any others known from the Trans-North China Orogen, it is difficult to place them in a regional context. However, two observations seem pertinent. Firstly, the fact that the first high-grade metamorphic event at 2770–2790 Ma occurred only ~50 Ma after magmatic crystallization is also a feature noted in the latest Neoproterozoic in NE China (Yang et al., 2008; Grant et al., this issue) where a mantle plume has been advocated as the source of heat driving the metamorphism. Further work in the Lushan area, particularly on the metamorphosed supracrustal rocks, is required to evaluate this. Secondly, the lack of evidence from this study of the meta-igneous rocks of a major metamorphic event at 1.85 Ga, as occurs throughout the northern and central parts of the Trans-North China Orogen (Zhao et al., 2005) and elsewhere at Lushan (Wan et al., 2006b), is significant. It would appear that the geology of Lushan is more complex than is evident from previous studies (Wan et al., 2006b; Yang et al., 2008) and that further work is required to resolve this matter.

Acknowledgements

We are grateful to H. Tao, H. Zhou and L.Q. Zhou for zircon CL imaging, Y.H. Zhang and Z.Q. Yang for assistance with zircon SHRIMP dating and F. Y. Wu, Y.H. Yang and L.W. Xie for help with the zircon Hf isotope analyses. A. Nutman is thanked for helpful discussions. The research was supported financially by the Key Program of the Ministry of Land and Resources of China (1212010711815), the Programs of the Beijing SHRIMP Center and of the State Key Laboratory of Lithospheric Evolution, Institute of Geology and Geophysics, Chinese Academy of Sciences. Wisc-SIMS is supported by the US National Science Foundation (EAR-0319230, -0516725, -0509639) and Department of Energy (93ER14389).

References

- Arth, J.G., Hanson, G.N., 1975. Geochemistry and origin of the early Precambrian crust of northeastern Minnesota. *Geochimica et Cosmochimica Acta* 39, 325–362.
- Black, L.P., Kamo, S.L., Allen, C.M., Aleinikoff, J.N., Davis, D.W., Korsch, R.J., Foudoulis, C., 2003. TEMORA 1: a new zircon standard for Phanerozoic U–Pb geochronology. *Chemical Geology* 200, 155–170.
- Blichert-Toft, J., Albarede, F., 1997. The Lu–Hf geochemistry of chondrites and the evolution of the mantle–crust system. *Earth and Planetary Science Letters* 148, 243–258.
- Chacko, T., Kumar, G.R., Meen, J.K., Rogers, J.J.W., 1992. Geochemistry of high-grade supracrustal rocks from the Kerala Khondalite Belt and adjacent massif charnockites, South India. In: van Reenen, D.D., Roering, C., Ashwal, L.D. (Eds.), *The Archaean Limpopo Granulite Belt: Tectonics and Deep Crustal Processes*. Precambrian Research, vol. 55, pp. 469–489.

- Chen, Y.J., 1996. Progress and problem: granulite terrane at the southern margin of the North China Craton. *Journal of Geology and Mineral Resources of North China* 11, 127–130 (in Chinese with English abstract).
- Dash, B., Sahu, K.N., Bowes, D.R., 1987. Geochemistry and original nature of Precambrian khondalites in the Eastern Ghats, Orissa, India. *Transactions of the Royal Society of Edinburgh* 78, 115–127.
- Grant, M.L., Wilde, S.A., Fuyuan Wu, F.Y., Yang, J.H., this issue. The application of zircon cathodoluminescence imaging, Th–U–Pb chemistry and U–Pb ages in interpreting discrete magmatic and high-grade metamorphic events in the North China Craton at the Archean/Proterozoic boundary. *Chemical Geology*.
- Hu, S.X., Lin, Q.L., Chen, Z.M., Sheng, Z.L., Li, S.M., 1988. The geology and metallogeny of the amalgamation zone between ancient North China plate and South China plate (taking Qinling-Tongbai as an example). Nanjing University Publishing House, Nanjing, pp. 59–60.
- Jahn, B.M., Glikson, A.Y., Peucat, J.J., Hickman, A.H., 1981. REE geochemistry and isotopic data of Archaean silicic volcanics and granitoids from the Pilbara Block, western Australia: implications for the early crustal evolution. *Geochimica et Cosmochimica Acta* 45, 1633–1652.
- Jahn, B.M., Auvray, B., Cornichet, J., Bai, Y.D., Shen, Q.H., Liu, D.Y., 1987. 3.5 Ga old amphibolites from eastern Hebei Province, China: field occurrence, petrography, Sm–Nd isochron age and REE geochemistry. *Precambrian Research* 34, 311–346.
- Jahn, B.M., Auvray, B., Shen, Q.H., Liu, D.Y., Zhang, Z.Q., Dong, Y.J., Ye, X.J., Zhang, Q.Z., Cornichet, J., Macé, J., 1988. Archean crustal evolution in China: the Taishan Complex, and evidence for juvenile crustal addition from long-term depleted mantle. *Precambrian Research* 38, 381–403.
- Jahn, B.M., Liu, D.Y., Wan, Y.S., Song, B., Wu, J.S., 2008. Archean crustal evolution of the Jiaodong peninsula, China, as revealed by zircon SHRIMP geochronology, elemental and Nd-isotope geochemistry. *American Journal of Science* 308, 232–269. doi:10.2475/03.2008.03.
- Kita, N.T., Ushikubo, T., Fu, B., Spicuzza, M.J., Valley, J.W., 2007. Analytical developments on oxygen three isotope analyses using a new generation ion microprobe IMS-1280. *Lunar and Planetary Science XXXVIII*, 1981.
- Kröner, A., Compston, W., Zhang, G.W., Guo, A.L., Todt, W., 1988. Age and tectonic setting of Late Archaean greenschist–gneiss terrain in Henan Province, China, as revealed by single-grain zircon dating. *Geology* 16, 211–215.
- Kröner, A., Cui, W.Y., Wang, S.Q., Wang, C.Q., Nemchin, A.A., 1998. Single zircon ages from high-grade rocks of the Jianping Complex, Liaoning Province, NE China. *Journal of Asian Earth Sciences* 16, 519–532.
- Kröner, A., Wilde, S.A., Li, J.H., Wang, K.Y., 2005. Age and evolution of a late Archaean to Paleoproterozoic upper to lower crustal section in the Wutaishan/Hengshan/Fuping terrain of northern China. *Journal of Asian Earth Sciences* 24, 577–595.
- Kröner, A., Wilde, S.A., Zhao, G.C., O'Brien, P.J., Sun, M., Liu, D.Y., Wan, Y.S., Liu, S.W., Guo, J.H., 2006. Zircon geochronology and metamorphic evolution of mafic dykes in the Hengshan Complex of northern China: evidence for late Palaeoproterozoic extension and subsequent high-pressure metamorphism in the North China Craton. *Precambrian Research* 146, 45–67.
- Liu, D.Y., Nutman, A.P., Compston, W., Wu, J.S., Shen, Q.H., 1992. Remnants of 3800 Ma crust in the Chinese part of the Sino-Korean craton. *Geology* 20, 339–342.
- Liu, D.Y., Wan, Y.S., Wu, J.S., Wilde, S.A., Zhou, H.Y., Dong, C.Y., Yin, X.Y., 2007. Eoarchean rocks and zircons in the North China Craton. In: van Kranendonk, M.J., Smithies, R.H., Bennett, V. (Eds.), *Earth's oldest Rocks*. Developments in Precambrian Geology, vol. 15. Elsevier, pp. 251–273.
- Ludwig, K.R., 2001a. Squid 1.02: A User's Manual, vol. 2. Special Publication, vol. 1b. Berkeley Geochronology Centre. 19 pp.
- Ludwig, K.R., 2001b. Users Manual for Isoplot/Ex (rev. 2.49): A Geochronological Toolkit for Microsoft Excel. Special Publication, vol. 1a. Berkeley Geochronology Center. 55pp.
- Martin, H., Smithies, R.H., Rapp, R., Moyen, J.F., Champion, D., 2005. An overview of adakite, tonalite–trondhjemite–granodiorite (TTG), and sanukitoid: relationships and some implications for crustal evolution. *Lithos* 79, 1–24.
- Page, F.Z., Ushikubo, T., Kita, N.T., Riciputi, L.R., Valley, J.W., 2007. High precision oxygen isotope analysis of picogram samples reveals 2- μm gradients and slow diffusion in zircon. *American Mineralogist* 92, 1772–1775.
- Santosh, M., Wilde, S.A., Li, J.H., 2007. Timing of Palaeoproterozoic ultrahigh-temperature metamorphism in the North China Craton: Evidence from SHRIMP U–Pb zircon geochronology. *Precambrian Research* 159, 178–196.
- Scherer, E., Munker, C., Mezger, K., 2001. Calibration of the Lutetium–Hafnium clock. *Science* 293, 683–687.
- Shen, Q.H., Geng, Y.S., Song, B., Wan, Y.S., 2005. New information from the surface outcrops and deep crust of Archaean Rocks of the North China and Yangtze Blocks, and Qinling–Dabie Orogenic Belt. *Acta Geologica Sinica* 79, 616–627 (in Chinese with English abstract).
- Song, B., Nutman, A.P., Liu, D.Y., Wu, J.S., 1996. 3800 to 2500 Ma crust in the Anshan area of Liaoning Province, northeastern China. *Precambrian Research* 78, 79–94.
- Sun, S.S., McDonough, W.F., 1989. Chemical and isotopic systematics of oceanic basalts: implications for mantle composition and processes. In: Saunders, A.D., Norry, M.J. (Eds.), *Magmatism in the Ocean Basins*. Special Publication, vol. 42. Geological Society of London, pp. 313–345.
- Steiger, R.H., Jaeger, E., 1977. Subcommittee on geochronology: convention on the use of decay constants in geo- and cosmochronology. *Earth and Planetary Science Letters* 36, 359–362.

Notes to Table 5:

Note: 1) Mg means magmatic zircons, Me-I, Me-II and Me-III represent zircons formed during the first, second and third metamorphic events, respectively.

2) $^{176}\text{Hf}/^{177}\text{Hf}(c)$ is $^{176}\text{Hf}/^{177}\text{Hf}$ corrected using standard 95100. The numbers in the second column are the SHRIMP dates and are the same as in Table 3; Age is in Ma. For all the samples (LS0417-1, LS0417-3, LS0417-2 and LS0417-4), t in $\epsilon_{\text{Hf}(T)}$ is the weighted mean $^{207}\text{Pb}/^{206}\text{Pb}$ age for the various domains in each sample. Zircon domains were identified using internal structures, compositions and ages. $T_{\text{DM}}(\text{Hf})$ values are single-stage model Hf ages.

- Valley, J.W., Lackey, J.S., Cavosie, A.J., Clechenko, C.C., Spicuzza, M.J., Basei, M.A.S., Bindeman, I.N., Ferreira, V.P., Sial, A.N., King, E.M., Peck, W.H., Sinha, A.K., Wei, C.S., 2005. 4.4 billion years of crustal maturation: oxygen isotopes in magmatic zircon. *Contributions to Mineralogy and Petrology* 150, 561–580.
- Vavra, G., Gebauer, D., Schmid, R., Compston, W., 1996. Multiple zircon growth and recrystallization during polyphase Late Carboniferous to Triassic metamorphism in granulites of the Ivrea Zone (Southern Alps): an ion microprobe (SHRIMP) study. *Contributions to Mineralogy and Petrology* 122, 337–358.
- Wan, Y.S., Song, B., Yang, C., Liu, D.Y., 2005a. Zircon SHRIMP U–Pb geochronology of Archean rocks from the Fushun–Qingyuan area, Liaoning Province and its geological significance. *Acta Geologica Sinica* 79, 78–87 (in Chinese with English abstract).
- Wan, Y.S., Liu, D.Y., Song, B., Wu, J.S., Yang, C.H., Zhang, Z.Q., Geng, Y.S., 2005b. Geochemical and Nd isotopic compositions of 3.8 Ga meta-quartz dioritic and trondhjemitic rocks from the Anshan area and their geological significance. *Journal of Asian Earth Sciences* 24, 563–575.
- Wan, Y.S., Li, R.W., Wilde, S.A., Liu, D.Y., Chen, Z.Y., Yan, L., Song, T.R., Yin, X.Y., 2005c. UHP metamorphism and exhumation of the Dabie Orogen, China: Evidence from SHRIMP dating of zircon and monazite from a UHP granitic gneiss cobble from the Hefei Basin. *Geochimica et Cosmochimica Acta* 69, 4333–4348.
- Wan, Y.S., Song, B., Liu, D.Y., Wilde, S.A., Wu, J.S., Shi, Y.R., Yin, X.Y., Zhou, H.Y., 2006a. SHRIMP U–Pb zircon geochronology of Palaeoproterozoic metasedimentary rocks in the North China Craton: evidence for a major Late Palaeoproterozoic tectonothermal event. *Precambrian Research* 149, 249–271.
- Wan, Y.S., Wilde, S.A., Liu, D.Y., Yang, C.X., Song, B., Yin, X.Y., 2006b. Further evidence for ~1.85 Ga metamorphism in the Central Zone of the North China Craton: SHRIMP U–Pb dating of zircon from metamorphic rocks in the Lushan area, Henan Province. *Gondwana Research* 9, 189–197.
- Wiedenbeck, M., Hancher, J.M., Peck, W.H., Sylvester, P., Valley, J., Whitehouse, M., Kronz, A., Morishita, Y., Nasdala, L., 2004. Further characterization of the 91500 zircon crystal. *Geostandards and Geoanalytical Research* 28, 9–39.
- Wilde, S.A., Cawood, P.A., Wang, K.Y., Nemchin, A.A., 2005. Granitoid evolution in the Late Archean Wutai Complex, North China Craton. *Journal of Asian Earth Sciences* 24, 597–613.
- Williams, I.S., 1998. U–Th–Pb geochronology by ion microprobe, applications of microanalytical techniques to understanding mineralizing processes. In: McKibben, M.A., Shanks, W.C., Ridley, W.I. (Eds.), *Reviews in Economic Geology*, vol. 7, pp. 1–35.
- Woodhead, J., Hergt, J., Shelley, M., Eggins, S., Kemp, R., 2004. Zircon HF-isotope analysis with an excimer laser, depth profiling, ablation of complex geometries, and concomitant age estimation. *Chemical Geology* 209, 121–135.
- Wu, F.Y., Zhao, G.C., Wilde, S.A., Sun, D.Y., 2005. Nd isotopic constraints on crustal formation in the North China Craton. *Journal of Asian Earth Sciences* 24, 523–545.
- Wu, F.Y., Yang, Y.H., Xie, L.W., Yang, J.H., Xu, P., 2006. Hf isotopic compositions of the standard zircons and baddeleyites used in U–Pb geochronology. *Chemical Geology* 44, 105–126.
- Yang, C.X., 2008. SHRIMP U–Pb zircon ages of the Early Precambrian metamorphic rocks and their geochemical characteristics in Lushan, Henan. *Geological Bulletin of China* 27, 517–533 (in Chinese with English abstract).
- Yang, J.H., Wu, F.Y., Wilde, S.A., 2008. Petrogenesis and geodynamics of Late Archean magmatism in the eastern North China Craton: geochronological, geochemical and Nd–Hf isotopic evidence. *Precambrian Research* 167, 125–149.
- Zhang, G.W., Bai, Y.B., Sun, Y., Guo, A.L., Zhou, D.W., Li, T.H., 1985. Composition and evolution of the Archean crust in central Henan, China. *Precambrian Research* 27, 7–35.
- Zhao, G.C., Wilde, S.A., Cawood, P.A., Lu, L.Z., 1998. Thermal evolution of Archean basement rocks from the eastern part of the North China craton and its bearing on tectonic setting. *International Geology Review* 40, 706–721.
- Zhao, G.C., Wilde, S.A., Cawood, P.A., Lu, L.Z., 1999. Thermal evolution of two-types of granulites from the North China Craton: evidence for both plume tectonics and collisional tectonics. *Geological Magazine* 139, 223–240.
- Zhao, G.C., Sun, M., Wilde, S.A., Li, S.Z., 2005. Late Archean to Paleoproterozoic evolution of the North China Craton: key issues revisited. *Precambrian Research* 136, 177–202.
- Zhou, D.W., Su, L., Jian, P., Wang, R.S., Liu, X.M., Lu, G.X., Wang, J.L., 2004. Zircon U–Pb SHRIMP ages of high-pressure granulite in Yushugou ophiolitic terrane in southern Tianshan and their tectonic implications. *Chinese Science Bulletin* 49, 1415–1419.